

---

# SafEDMD: A certified learning architecture tailored to data-driven control of nonlinear dynamical systems

---

**Robin Strässer**

Institute for Systems Theory  
and Automatic Control  
University of Stuttgart  
70550 Stuttgart, Germany  
straesser@ist.uni-stuttgart.de

**Manuel Schaller**

Institute for Mathematics  
Technische Universität Ilmenau  
99693 Ilmenau, Germany  
manuel.schaller@tu-ilmenau.de

**Karl Worthmann**

Institute for Mathematics  
Technische Universität Ilmenau  
99693 Ilmenau, Germany  
karl.worthmann@tu-ilmenau.de

**Julian Berberich**

Institute for Systems Theory  
and Automatic Control  
University of Stuttgart  
70550 Stuttgart, Germany  
berberich@ist.uni-stuttgart.de

**Frank Allgöwer**

Institute for Systems Theory  
and Automatic Control  
University of Stuttgart  
70550 Stuttgart, Germany  
allgower@ist.uni-stuttgart.de

## Abstract

The Koopman operator serves as the theoretical backbone for machine learning of dynamical control systems, where the operator is heuristically approximated by extended dynamic mode decomposition (EDMD). In this paper, we propose Stability- and certificate-oriented EDMD (SafEDMD): a novel EDMD-based learning architecture which comes along with rigorous certificates, resulting in a reliable surrogate model generated in a data-driven fashion. To ensure the trustworthiness of SafEDMD, we derive proportional error bounds, which vanish at the origin and are tailored to control tasks, leading to certified controller design based on semi-definite programming. We illustrate the developed method by means of several benchmark examples and highlight the advantages over state-of-the-art methods.

## 1 Introduction

Extended dynamic mode decomposition (EDMD; [1]) is one of the most popular machine learning algorithms to learn highly nonlinear dynamical (control) systems from data. Its applications range from climate forecasting [2], over electrocardiography [3] to quantum mechanics [4], cryptography [5], and nonlinear fluid dynamics [6]. The strength of EDMD lies in its analytical foundation by means of the Koopman operator, which *propagates* observable functions (e.g., measurement sensors) along the flow of the underlying dynamical system. As the Koopman operator acts linearly on observables, EDMD leverages tools from regression to efficiently learn this linear object on a finite-dimensional set of observables, which renders the implementation of this learning algorithm

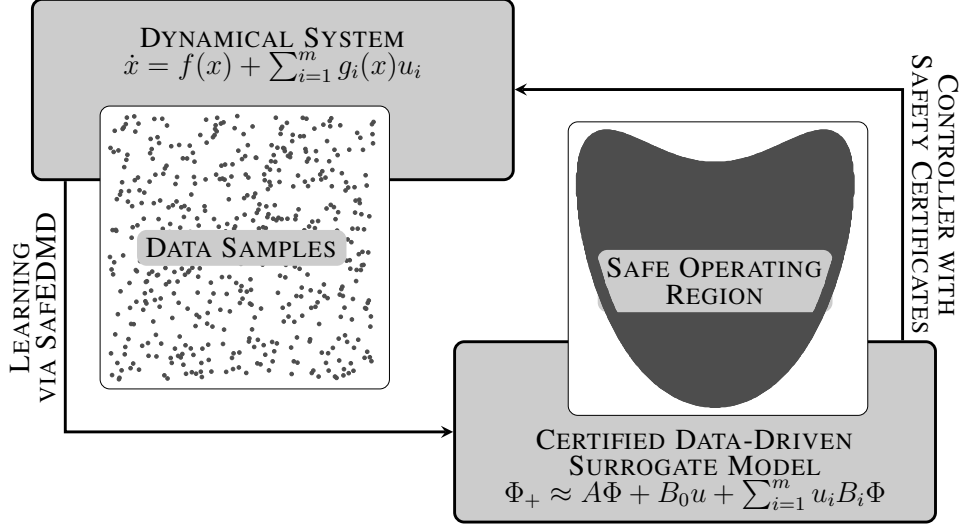


Figure 1: Illustration of the proposed learning architecture SafEDMD tailored to certified data-driven control. The proposed approach first learns a bilinear surrogate model of the unknown nonlinear system based on data samples along with rigorous error bounds. Next, a controller is designed which exploits the model and the guaranteed error bounds to reliably control the nonlinear system in a SOR.

relatively straightforward. Moreover, advanced tools from operator theory and linear regression enable certification of this machine learning algorithm [7, 8]. For control tasks, in particular in safety-critical applications, such certificates are key [9]. The EDMD algorithm can be extended to control systems in order to take advantage of the reliability and strong analytical foundation. Two algorithms are predominantly used throughout the literature, namely EDMDc [10, 11] and bilinear EDMD [12, 13], where a linear and bilinear model is learned, respectively. As such, EDMD with control has been extensively and successfully used in various applications, see [14] and the references therein.

The reliable control of complex systems based on EDMD requires certificates on the learning algorithm. To this end, [15] proved convergence of EDMD to the Koopman operator in the infinite-data limit. Finite-data error bounds were proven in [16] and [17] for deterministic systems based on ergodic and i.i.d. sampling, respectively, and further refined in [18] under less-restrictive assumptions including discrete-time systems. The first extension to (stochastic) control systems is given in [19] including error bounds for bilinear EDMD. The error bounds in these works, however, are global in the sense that the error does not vanish at the origin, which prevents a straightforward application of standard control methods.

In this work, we present **Stability- and certificate-oriented EDMD (SafEDMD)** - a learning architecture with rigorous certificates, which is tailored to data-driven control of nonlinear systems. The architecture relies on a structured EDMD algorithm to learn a bilinear surrogate model of a nonlinear system based on data samples. To enable reliable controller design, SafEDMD is accompanied by bounds on its approximation error which, in contrast to existing results, vanish at the origin. This enables the design of safe controllers, which we illustrate with the exemplary control objective of stabilization in a safe operating region (SOR). While some concepts are connected to [20, 21], the key difference is that the proposed approach handles the Koopman operator directly in the discrete-time domain using sampled data of the system. Contrary, [20, 21] work with the corresponding *generator*, requiring time-derivative data, which are hard to obtain and typically significantly noisier in practice. To the best of our knowledge, the proposed approach is the first to control unknown nonlinear systems based on derivative-free data using the Koopman operator while giving rigorous stability certificates.

The overall approach is illustrated in Figure 1 with the main contributions summarized as follows:

- (1) We propose SafEDMD – a novel certified and highly efficient architecture for machine learning with EDMD particularly suited for control tasks.
- (2) We rigorously derive certified error bounds tailored to controller design.

- (3) To illustrate the applicability of the proposed learning architecture and its error bounds, we exemplarily design a feedback controller and provide a certificate for the successful completion of the stabilization task.
- (4) We illustrate the methodology with various examples, highlighting scenarios where the proposed architecture allows to successfully learn and control unknown nonlinear systems whereas existing methods fail.

The paper is organized as follows. In Section 2, we recall the notion of the Koopman operator and its representation of nonlinear dynamical systems. Section 3 describes the framework SafEDMD introducing a certified learning architecture tailored to data-driven control. Section 4 illustrates the applicability of SafEDMD for control tasks, where we design a certified data-driven feedback controller. Finally, Section 5 validates the proposed learning architecture as well as the controller design in numerical experiments.

## 2 The Koopman operator as foundation for certifiable learning of dynamical systems

In the following, we briefly recap the necessary background on the Koopman operator and its representation of nonlinear dynamical systems in Section 2.1. Then, in Section 2.2, we discuss a sampled-data Koopman representation in preparation for the proposed certified learning scheme.

### 2.1 Koopman representation of nonlinear dynamical systems

Throughout the paper, we consider *unknown* nonlinear control-affine systems of the form

$$\dot{x}(t) = f(x(t)) + \sum_{i=1}^m g_i(x(t))u_i(t), \quad (1)$$

where  $x(t) \in \mathbb{R}^n$  denotes the state at time  $t \geq 0$  and the control function  $u : [0, \infty) \rightarrow \mathbb{R}^m$  serves as an input. The map  $f : \mathbb{R}^n \rightarrow \mathbb{R}^n$  is called drift, while  $g_i : \mathbb{R}^n \rightarrow \mathbb{R}^n$ ,  $i \in [m]$ , are called input maps<sup>1</sup>. For an initial condition  $x(0) = \hat{x} \in \mathbb{R}^n$  and a control function  $u$ , we denote the solution of (1), provided it exists, at time  $t \geq 0$  by  $x(t; \hat{x}, u)$ . We assume that  $f(0) = 0$  holds, i.e., the origin is a controlled equilibrium for  $u = 0$ .

The Koopman operator  $\mathcal{K}_t^u$  introduced in [22] provides a powerful alternative representation of the nonlinear dynamical system (1) through the lens of observable functions given by, e.g., measurements in a particular application. More precisely, the Koopman operator  $\mathcal{K}_t^u$  corresponding to (1) with constant input  $u(t) \equiv u \in \mathbb{U}$  for a compact set  $\mathbb{U} \subseteq \mathbb{R}^m$  with  $0 \in \text{int}(\mathbb{U})$  is defined as

$$(\mathcal{K}_t^u \varphi)(\hat{x}) = \varphi(x(t; \hat{x}, u)) \quad (2)$$

for all  $t \geq 0$ ,  $\hat{x} \in \mathbb{X}$ ,  $\varphi \in L^2(\mathbb{X}, \mathbb{R})$ , where  $\mathbb{X} \subseteq \mathbb{R}^n$  is a compact set and the real-valued functions  $\varphi$  are called *observables*.<sup>2</sup> As the Koopman operator  $\mathcal{K}_t^u$  is an infinite-dimensional, but *linear* operator on observable functions  $\varphi$ , it enables the use of powerful data-driven techniques for learning such as, e.g., linear regression.

As shown in, e.g., in [24, 20, 25], the Koopman operator  $\mathcal{K}_t^u$  inherits the control-affine structure of (1) *approximately*, i.e.,

$$\mathcal{K}_t^u \approx \mathcal{K}_t^0 + \sum_{i=1}^m u_i (\mathcal{K}_t^{e_i} - \mathcal{K}_t^0) \quad (3)$$

holds, where  $\mathcal{K}_t^0$  and  $\mathcal{K}_t^{e_i}$ ,  $i \in [m]$ , are the Koopman operators corresponding to the constant control functions  $u \equiv 0$  and  $u \equiv e_i$  with unit vectors  $e_i$ ,  $i \in [m]$ , respectively. The resulting approximation error is precisely investigated in Theorem 3.1.

The core of data-driven techniques leveraging the Koopman operator, such as EDMD as discussed later, is to learn the action of the Koopman operator on a subspace, called the *dictionary*. To this

<sup>1</sup>In this paper, we use  $[a : b] := \mathbb{Z} \cap [a, b]$  and  $[b] := [1 : b]$ .

<sup>2</sup>We tacitly assumed invariance of  $\mathbb{X}$  under the flow such that the observable functions are defined on  $x(t; \hat{x}, u)$  for all  $\hat{x} \in \mathbb{X}$ , which can be relaxed by considering initial values in a tightened version of  $\mathbb{X}$ , see, e.g., [23].

end, we define the dictionary  $\mathbb{V} := \text{span}\{\phi_\ell\}_{\ell=0}^N$  representing the  $(N + 1)$ -dimensional subspace spanned by the chosen observables  $\phi_0 \equiv 1$  and  $\phi_\ell \in \mathcal{C}^1(\mathbb{R}^n, \mathbb{R})$  with  $\phi_\ell(0) = 0$ ,  $\ell \in [N]$ . In particular, we choose the observables

$$\Phi(x) = [1 \quad x^\top \quad \phi_{n+1}(x) \quad \cdots \quad \phi_N(x)]^\top. \quad (4)$$

Note that

$$\|x\| \leq \|\Phi(x) - \Phi(0)\| \leq L_\Phi \|x\|, \quad (5)$$

where the first inequality follows since  $\Phi$  explicitly contains  $x$ , and the second inequality follows from local Lipschitz continuity due to  $\Phi \in \mathcal{C}^1(\mathbb{R}^n, \mathbb{R}^N)$ . Common choices for the observables  $\Phi$  include monomials or radial basis functions such as, e.g., thin-plate splines. If prior knowledge about the system dynamics is available, suitable observables can often be inferred from the system dynamics, see, e.g., [26] or [27] for an approach to construct a dictionary tailored to robotic systems. Although not explicitly considered in this paper, the observables  $\phi_\ell$ ,  $\ell \in [n + 1, N]$ , can also be learned via a neural network (NN). Parametrizing  $\Phi$  by an NN increases the expressiveness and allows finding suitable nonlinear observables  $\phi_\ell$  for the underlying system dynamics (1), see, e.g., [28]. Here, the assumed Lipschitz continuity in (5) of the learned NN can be ensured by design [29].

In (4), we assume that the full state is contained in the dictionary. Preliminary results, however, motivate that dictionaries being observable from a system-theoretic point of view may suffice to design a stabilizing controller, where the state coordinates are reconstructed via, e.g., delay coordinates [30]. A rigorous investigation of non-state-inclusive dictionaries is left for future work.

## 2.2 Sampled-data Koopman representation

When controlling dynamical systems of the form (1), a direct implementation of a (piecewise) continuous control function  $u : [0, \infty) \rightarrow \mathbb{R}^m$  is typically not feasible. Instead, a common strategy is to sample the system (1), e.g., equidistantly in time, and consider piecewise constant control inputs on each interval, i.e.,  $u(t) \equiv u_k \in \mathbb{U}$  holds for all  $t \in [t_k, t_k + \Delta t)$  with sampling period  $\Delta t > 0$  and  $t_k = k\Delta t$ ,  $k \in \mathbb{N}_0$ . This leads to the discretized system representation

$$x_{k+1} = x_k + \int_{t_k}^{t_k + \Delta t} f(x(t)) + \sum_{i=1}^m g_i(x(t))(u_k)_i dt \quad (6)$$

with  $x(t) = x(t; \hat{x}, u)$  and  $x_k = x(t_k; \hat{x}, u)$ . From (2), we deduce the discrete-time Koopman representation

$$\Phi(x_{k+1}) = (\mathcal{K}_{\Delta t}^u \Phi)(x_k). \quad (7)$$

Note that the evolution of  $\Phi(x_k)$  allows to retrieve the underlying state  $x$  by projection due to the choice of the lifting function  $\Phi$  in (4), such that  $x = [0_{n \times 1} \quad I_n \quad 0_{n \times N-n}] \Phi(x)$  by definition.

## 3 SafEDMD: a certified learning architecture tailored to nonlinear dynamical systems

In the following, we present a tailored learning architecture for nonlinear systems based on the Koopman operator particularly suited for certifiability in control tasks. Since the true nonlinear system dynamics are unknown, we leverage the linearity of the Koopman operator in the observables to learn a certifiable data-driven approximation. More precisely, we introduce a novel learning architecture called *SafEDMD*. This framework 1) learns a data-based bilinear surrogate model of the Koopman operator solely relying on linear regression and 2) ensures error certificates that allow the usage of the surrogate model for reliable control tasks, e.g., closed-loop stabilization.

In order to determine data-driven estimates of  $\mathcal{K}_{\Delta t}^u$  for constant control inputs  $u(t) \equiv \bar{u}$  for  $\bar{u} \in \{0, e_1, \dots, e_m\}$ , we consider data samples  $\mathcal{D} = \{x_j^{\bar{u}}, y_j^{\bar{u}}\}_{j=1}^{d^{\bar{u}}}$ , where  $y_j^{\bar{u}} = x(\Delta t; x_j^{\bar{u}}, \bar{u})$  and the control inputs  $e_i$ ,  $i \in [m]$ , are the unit vectors. In particular, we need no information about the state derivative but only require trajectory samples of the state and its successor of unknown nonlinear system (1) for a set of chosen control values.

The proposed learning approach crucially exploits that the Koopman operator acting on the defined lifting function  $\Phi$  has a specific structure. In particular, note that  $\Phi$  contains a constant observable

$\phi_0 \equiv 1$ , i.e.,  $\phi_0(x_{k+1}) = \phi_0(x_k) = 1$ , and, thus,  $\Phi(0) = (\mathcal{K}_{\Delta t}^0 \Phi)(0)$  due to  $f(0) = 0$ . Therefore, using (3), we partition the function space into constant functions and the remainder to obtain

$$\mathcal{K}_{\Delta t}^u = \begin{bmatrix} 1 & 0 \\ (\mathcal{K}_{\Delta t}^u)_{21} & (\mathcal{K}_{\Delta t}^u)_{22} \end{bmatrix}, \quad \mathcal{K}_{\Delta t}^0 = \begin{bmatrix} 1 & 0 \\ 0 & (\mathcal{K}_{\Delta t}^0)_{22} \end{bmatrix}, \quad \mathcal{K}_{\Delta t}^{e_i} = \begin{bmatrix} 1 & 0 \\ (\mathcal{K}_{\Delta t}^{e_i})_{21} & (\mathcal{K}_{\Delta t}^{e_i})_{22} \end{bmatrix} \quad (8)$$

as the corresponding partition of the Koopman operators. Due to the structure of the Koopman operator in (8), we enforce the same structure for the data-driven surrogates in our proposed architecture, i.e., we adopt the structure in the finite-dimensional model given by

$$\mathcal{K}_{\Delta t, d}^0 = \begin{bmatrix} 1 & 0 \\ 0 & A \end{bmatrix}, \quad \mathcal{K}_{\Delta t, d}^{e_i} = \begin{bmatrix} 1 & 0 \\ B_{0,i} & \hat{B}_i \end{bmatrix}. \quad (9)$$

To learn the unknown matrices  $A$ ,  $B_{0,i}$ ,  $\hat{B}_i$ , we arrange the data  $\mathcal{D}$  in

$$X^0 = [0_{N \times 1} \quad I_N] [\Phi(x_1^0) \quad \cdots \quad \Phi(x_{d_0}^0)], \quad X^{e_i} = [\Phi(x_1^{e_i}) \quad \cdots \quad \Phi(x_{d^{e_i}}^{e_i})], \quad (10a)$$

$$Y^{\bar{u}} = [0_{N \times 1} \quad I_N] [\Phi(y_1^{\bar{u}}) \quad \cdots \quad \Phi(y_{d^{\bar{u}}}^{\bar{u}})]. \quad (10b)$$

The proposed learning architecture relies on solving the linear regression problems

$$A = \arg \min_{A \in \mathbb{R}^{N \times N}} \|Y^0 - AX^0\|_F, \quad [B_{0,i} \quad \hat{B}_i] = \arg \min_{\substack{B_{0,i} \in \mathbb{R}^N, \\ \hat{B}_i \in \mathbb{R}^{N \times N}}} \|Y^{e_i} - [B_{0,i} \quad \hat{B}_i] X^{e_i}\|_F \quad (11)$$

for  $i \in [m]$ , where  $\|\cdot\|_F$  denotes the Frobenius norm. Based on the estimates in (11), we can construct a data-driven surrogate model for the discretization of the nonlinear dynamical system (1), i.e.,  $\mathcal{K}_{\Delta t, d}^u = \mathcal{K}_{\Delta t, d}^0 + \sum_{i=1}^m u_i (\mathcal{K}_{\Delta t, d}^{e_i} - \mathcal{K}_{\Delta t, d}^0)$ . This model, however, is only an approximation of the true Koopman operator in (7), meaning that

$$\Phi(x_{k+1}) \approx \mathcal{K}_{\Delta t, d}^u \Phi(x_k). \quad (12)$$

The error is due to the different sources, including the bilinear approximation (3) as well as the above data-driven estimation. In the following main result, which forms the foundation of the proposed learning architecture, we provide a rigorous analysis of this error.

**Theorem 3.1.** *Suppose that the data samples  $\mathcal{D}$  are i.i.d. Then, for any probabilistic tolerance  $\delta \in (0, 1)$ , amount of data  $d_0 \in \mathbb{N}$  and sampling rate  $\Delta t > 0$ , there are constants  $\bar{c}_x, \bar{c}_u = \mathcal{O}(1/\sqrt{\delta d_0} + \Delta t^2)$  such that for all  $d \geq d_0$ , the learning error bound<sup>3</sup>*

$$\|(P_{\mathbb{V}} \mathcal{K}_{\Delta t}^u|_{\mathbb{V}}) \Phi(x) - \mathcal{K}_{\Delta t, d}^u \Phi(x)\| \leq \bar{c}_x \|\Phi(x) - \Phi(0)\| + \bar{c}_u \|u\| \quad (13)$$

holds for all  $x \in \mathbb{X}$  and  $u \in \mathbb{U}$  with probability  $1 - \delta$ .

*Proof (Sketch).* We prove the result in two steps, see Appendix A for details. First, we bound the error of the bilinear representation for the projected Koopman operator  $P_{\mathbb{V}} \mathcal{K}_{\Delta t}^u|_{\mathbb{V}}$  in (3). Then, we incorporate the estimation error from learning the bilinearized Koopman operator from data.  $\square$

The error bound (13) of above Theorem 3.1 features two central ingredients crucial for design. The first aspect is that it is proportional in the sense that the right-hand side vanishes for  $(x, u) = 0$ . Such a proportional bound is, to the best of the authors' knowledge, so far not present in any learning scheme using the notably simple EDMD-framework and is decisive for controller design such that the underlying true system is reliably and safely operated by feedback control in a region containing the origin. The second point is that the proportionality constants  $\bar{c}_x$  and  $\bar{c}_u$  in (13) can be made arbitrarily small when choosing a sufficiently high amount of data points  $d_0$  and a small enough sampling rate  $\Delta t$ . This is important for a successful controller design since the considered safety objective requires robustness against all possible learning errors satisfying the bound in (13). While we consider i.i.d. sampling in this paper, future work should investigate proportional error bounds for other sampling strategies (e.g. ergodic sampling), where we conjecture that similar arguments as in Theorem 3.1 apply if the estimation error of the data-based Koopman estimate  $\|P_{\mathbb{V}} \mathcal{K}_{\Delta t}^u|_{\mathbb{V}} - \mathcal{K}_{\Delta t, d}^u\|$  is bounded. Further, motivated by the experiments conducted in Section 5, we expect that the result in Theorem 3.1 generalizes to the case of noisy data, see, e.g., [31] for related bounds on the Koopman estimate.

The following corollary provides a proportional bound on the complete approximation error, where an additional projection error due to a *finite* dictionary of observables is taken into account.

<sup>3</sup>  $P_{\mathbb{V}}$  denotes the  $L^2$ -orthogonal projection onto  $\mathbb{V}$ .

---

**Algorithm 1** SafEDMD: Certified learning architecture tailored to data-driven control of nonlinear dynamical systems

---

**Input:** data  $\mathcal{D} = \{x_j^{\bar{u}}, y_j^{\bar{u}}\}_{j=1}^d$  for  $\bar{u} = 0, e_1, \dots, e_m$  with  $y_j^{\bar{u}} = x(\Delta t; x_j^{\bar{u}}, \bar{u})$ , observables  $\Phi$   
 Arrange data in (10).  
 Solve (11).  
**Output:** certified Koopman representation (12) with  $\mathcal{K}_{\Delta t, d}^0, \mathcal{K}_{\Delta t, d}^{e_1}, \dots, \mathcal{K}_{\Delta t, d}^{e_m}$  defined in (9)

---

**Corollary 3.2.** *Let the assumptions of Theorem 3.1 hold. If there exists a proportional error bound on the projection error, i.e.,*

$$\|(\mathcal{K}_{\Delta t}^u \Phi)(x) - (P_{\mathbb{V}} \mathcal{K}_{\Delta t}^u|_{\mathbb{V}}) \Phi(x)\| \leq \tilde{c}_x \|\Phi(x) - \Phi(0)\| + \tilde{c}_u \|u\|, \quad (14)$$

then for any probabilistic tolerance  $\delta \in (0, 1)$ , amount of data  $d_0 \in \mathbb{N}$  and sampling rate  $\Delta t > 0$ , there are constants  $\bar{c}_x, \bar{c}_u = \mathcal{O}(1/\sqrt{\delta d_0} + \Delta t^2)$  such that for all  $d \geq d_0$ , the full approximation error  $\|(\mathcal{K}_{\Delta t}^u \Phi)(x) - \mathcal{K}_{\Delta t, d}^u \Phi(x)\|$  is proportionally bounded by

$$\|(\mathcal{K}_{\Delta t}^u \Phi)(x) - \mathcal{K}_{\Delta t, d}^u \Phi(x)\| \leq c_x \|\Phi(x) - \Phi(0)\| + c_u \|u\|, \quad (15)$$

for all  $x \in \mathbb{X}$  and  $u \in \mathbb{U}$  with probability  $1 - \delta$ , where  $c_x = \bar{c}_x + \tilde{c}_x$  and  $c_u = \bar{c}_u + \tilde{c}_u$ .

*Proof.* As a direct consequence of Theorem 3.1 and the triangle inequality, we compute

$$\begin{aligned} \|(\mathcal{K}_{\Delta t}^u \Phi)(x) - \mathcal{K}_{\Delta t, d}^u \Phi(x)\| &\leq \|(\mathcal{K}_{\Delta t}^u \Phi)(x) - (P_{\mathbb{V}} \mathcal{K}_{\Delta t}^u|_{\mathbb{V}}) \Phi(x)\| + \|((P_{\mathbb{V}} \mathcal{K}_{\Delta t}^u|_{\mathbb{V}}) - \mathcal{K}_{\Delta t, d}^u) \Phi(x)\| \\ &\leq (\bar{c}_x + \tilde{c}_x) \|\Phi(x) - \Phi(0)\| + (\bar{c}_u + \tilde{c}_u) \|u\|. \quad \square \end{aligned}$$

Note that the proportional bound (14) trivially holds if, e.g., the dictionary  $\mathbb{V}$  is invariant w.r.t. the dynamics, i.e.,  $P_{\mathbb{V}} \mathcal{K}_t^u|_{\mathbb{V}} = \mathcal{K}_t^u|_{\mathbb{V}}$ . This property is commonly employed in Koopman-based control [32, 33, 34, 35, 36, 37, 38]. Conditions for the (approximate) satisfaction of this invariance are given by, e.g., [32, 39, 37, 26]. Then, one has to additionally account for the projection error [40]. In [41, Sec. 4], the authors suggest to derive uniform bounds based on polynomial tests, where interpolation arguments may be used to ensure the proportional bound as in (14) on the projection error, see, e.g., [42, 43] for recently derived uniform error bounds w.r.t. autonomous systems.

The proposed learning architecture tailored to data-driven control of nonlinear dynamical systems based on the linear regression problems (11) and the error bound (15) is summarized in Algorithm 1.

## 4 Certified data-driven controller design for nonlinear systems

In this section, we use the certified learning architecture SafEDMD presented in Section 3 to design a safe controller for System (1). More precisely, our goal is to find a state-feedback controller  $\mu : \mathbb{R}^n \rightarrow \mathbb{R}^m$  exponentially stabilizing the setpoint in closed loop using the control input  $u_k = \mu(x_k)$ , i.e., it is stable [44] and trajectories exponentially converge to the setpoint. Without loss of generality, we assume that the setpoint is the origin  $x = 0$ . To find a suitable controller, we first proceed as in Algorithm 1 to obtain a data-driven surrogate model of the unknown nonlinear system based on sampled data. We then use this model along with the error bound in Corollary 3.2 to design a data-driven controller with a stability certificate. The overall control scheme is illustrated in Figure 2.

To obtain rigorous safety guarantees, our proposed controller ensures that the system trajectories evolve in a predetermined set  $\Delta_{\Phi} = \{\psi \in \mathbb{R}^N \mid (16) \text{ holds}\}$  with

$$\begin{bmatrix} \psi \\ 1 \end{bmatrix}^{\top} \begin{bmatrix} Q_z & S_z \\ S_z^{\top} & R_z \end{bmatrix} \begin{bmatrix} \psi \\ 1 \end{bmatrix} \geq 0 \quad (16)$$

for fixed matrices  $Q_z \in \mathbb{R}^{N \times N}$ ,  $S_z \in \mathbb{R}^N$ ,  $R_z \in \mathbb{R}$  with  $Q_z \prec 0$  and  $R_z > 0$  for which the inverse  $\begin{bmatrix} \bar{Q}_z & \bar{S}_z \\ \bar{S}_z^{\top} & \bar{R}_z \end{bmatrix} := \begin{bmatrix} Q_z & S_z \\ S_z^{\top} & R_z \end{bmatrix}^{-1}$  exists. In particular, we enforce  $\hat{\Phi}(x) \in \Delta_{\Phi}$  for all times, where  $\hat{\Phi} := [0_{N \times 1} \quad I_N] \Phi(x)$  denotes the reduced observable function after removing the constant observable  $\phi_0 \equiv 1$  such that  $\hat{\Phi}(0) = 0$ . The parametrization of  $\Delta_{\Phi}$  includes, e.g., a simple norm

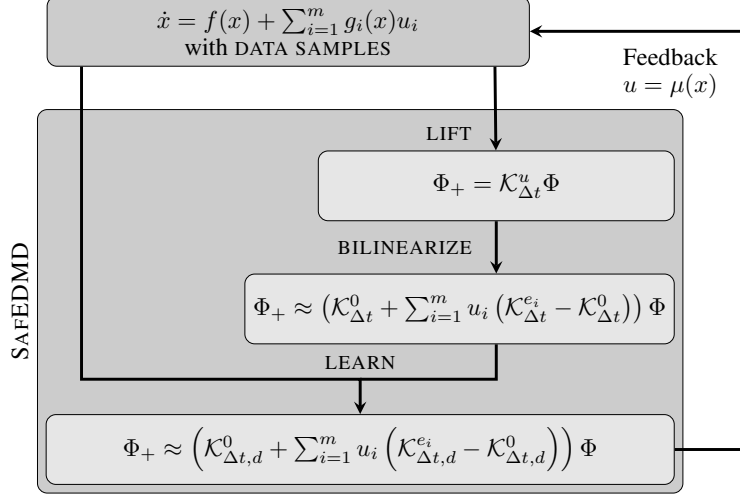


Figure 2: Certified data-driven controller design for nonlinear dynamical systems. The overall scheme consists of two main steps: 1) learning a certified surrogate model along with error bounds using SafEDMD; 2) designing a feedback controller  $u = \mu(x)$  which robustly stabilizes the surrogate model. The approach yields reliable safety guarantees due to the rigorous foundation based on SafEDMD, which learns a bilinear approximation of the Koopman operator dynamics using data.

bound  $\|\hat{\Phi}(x)\|^2 \leq c$  for all  $x$  by choosing  $Q_z = -I$ ,  $S_z = 0$ , and  $R_z = c$ . More sophisticated parametrizations are also possible by including prior knowledge of the system or using heuristics (compare [21, Sec. V]). The set  $\Delta_\Phi$  needs to be defined by the user before applying the following controller design procedure. Ideally, one chooses  $\Delta_\Phi$  preferably large since it determines an outer bound on the SOR in which the proposed controller reliably controls the system. However, there is a trade-off since too large choices of  $\Delta_\Phi$  may lead to an infeasible controller design. In Section 5, we discuss practical possibilities for choosing  $\Delta_\Phi$  using numerical examples.

The following theorem yields a controller-design method guaranteeing safe operation and exponential stability of the *sampled* nonlinear system (6) by solving a linear matrix inequality feasibility problem.

**Theorem 4.1.** *Let the data points  $\mathcal{D}$  be sampled i.i.d. from  $\mathbb{X}$ . Suppose a data-driven surrogate model of the unknown nonlinear system (1) as learned using the certified learning architecture defined in Algorithm 1 satisfying the error bound Corollary 3.2 with given probabilistic tolerance  $\delta \in (0, 1)$ , sampling rate  $\Delta t > 0$ , and constants  $c_x, c_u = \mathcal{O}(1/\sqrt{\delta d_0} + \Delta t^2)$ .*

*Further, assume there is a matrix  $0 \prec P = P^\top \in \mathbb{R}^{N \times N}$ , matrices  $L \in \mathbb{R}^{m \times N}$ ,  $L_w \in \mathbb{R}^{m \times Nm}$ , a matrix  $0 \prec \Lambda = \Lambda^\top \in \mathbb{R}^{m \times m}$ , and scalars  $\nu > 0$ ,  $\tau > 0$  such that*

$$\begin{bmatrix} P - \tau I_N & -\tilde{B}(\Lambda \otimes \tilde{S}_z) - B_0 L_w (I_m \otimes \tilde{S}_z) & 0 & AP + B_0 L & \tilde{B}(\Lambda \otimes I_N) + B_0 L_w \\ * & (\Lambda \otimes \tilde{R}_z) - L_w (I_m \otimes \tilde{S}_z) - (I_m \otimes \tilde{S}_z^\top) L_w^\top & -(I_m \otimes \tilde{S}_z^\top) \begin{bmatrix} 0 \\ L_w \end{bmatrix} & L & L_w \\ * & * & 0.5\tau \begin{bmatrix} c_x^{-2} I_N & 0 \\ 0 & c_u^{-2} I_m \end{bmatrix} & \begin{bmatrix} P \\ L \end{bmatrix} & -\begin{bmatrix} 0 \\ L_w \end{bmatrix} \\ * & * & * & P & 0 \\ * & * & * & * & -(\Lambda \otimes \tilde{Q}_z^{-1}) \end{bmatrix} \succ 0, \quad (17)$$

$$\begin{bmatrix} \nu \tilde{R}_z - 1 & -\nu \tilde{S}_z^\top \\ -\nu \tilde{S}_z & \nu \tilde{Q}_z + P \end{bmatrix} \preceq 0 \quad (18)$$

*hold. Then there exists an amount of data  $d_0 \in \mathbb{N}$  such that for all  $d \geq d_0$  the controller<sup>4</sup>*

$$\mu(x) = (I - L_w(\Lambda^{-1} \otimes \hat{\Phi}(x)))^{-1} L P^{-1} \hat{\Phi}(x) \quad (19)$$

*ensures exponential stability of the sampled nonlinear system (6) for all initial conditions in the SOR  $\hat{x} \in \mathcal{X}_{\text{SOR}} := \{x \in \mathbb{R}^n \mid \hat{\Phi}(x)^\top P^{-1} \hat{\Phi}(x) \leq 1\}$  with probability  $1 - \delta$ .*

*Proof (Sketch).* The result is shown in two steps. First, we show that all  $x \in \mathcal{X}_{\text{SOR}}$  satisfy  $\hat{\Phi}(x) \in \Delta_\Phi$ . Then, we conclude positive invariance of  $\mathcal{X}_{\text{SOR}}$  together with exponential stability of the

<sup>4</sup>By  $\otimes$  we refer to the Kronecker product.

sampled closed-loop system (6) for all  $\hat{x} \in \mathcal{X}_{\text{SOR}}$ . This ensures safe operation under the obtained feedback via the certified learning architecture of Algorithm 1, see Appendix B for details.  $\square$

The proposed controller design in Theorem 4.1 is purely based on data samples of the state trajectory and does not rely on model knowledge. In particular, we use the certified learning scheme SafEDMD satisfying the error bound specified in Corollary 3.2 to obtain a reliable data-driven system parametrization. Learning the Koopman-based surrogate model via Algorithm 1 only requires solving the least-squares optimization problem (11), which scales well to higher-dimensional systems [45, 46]. The controller design approach, on the other hand, is framed as a semi-definite program using linear matrix inequalities with complexity  $\mathcal{O}(N^6)$ . Although efficiently solvable for a moderate dictionary size  $N$  [47], future work should be devoted to including structure-exploiting SDP techniques, see, e.g., [48, 49]. In Section 5, we show that the proposed approach can successfully control common benchmark systems in Koopman theory with more reliable behavior than existing approaches. The robust controller uses the learning error bounds in (15) to ensure safe operation of the resulting controller when applied to the unknown nonlinear system. Here, we can directly relate a given desired accuracy and certainty about the closed-loop guarantees as well as the input dimension  $m$  to the necessary amount of data  $d_0$  and the sampling period  $\Delta t$ .

We note that the controller parametrization (19) contains the control law  $\mu(x) = K\hat{\Phi}(x)$ , which is linear in the lifted state, as a special case for  $L_w = 0$  and  $K = LP^{-1}$ . However, our proposed nonlinear controller parametrization (19) achieves larger regions of safe operation  $\mathcal{X}_{\text{SOR}}$  for which we can guarantee reliable behavior in closed loop.

On a technical level, the controller design approach in Theorem 4.1 follows similar ideas as in [21]. The key difference of Theorem 4.1 to this existing work is that the latter designs a data-driven controller based on an estimate of the Koopman *generator*, i.e., it involves learning a continuous-time model and designing a controller, which continuously changes the respective control values. The key disadvantage of the proposed scheme in [21] is that derivative measurements are required, which limits its practical use, especially in the presence of noisy data. Instead, here, Theorem 4.1 relies on a discrete-time controller design for the sampled nonlinear system with sample-and-hold implementation of the control signal (6) (compare [50, 51]). The main contribution of the introduced controller design is the tight connection to the SafEDMD learning architecture and, hence, it leads to reliable and certified guarantees for the true nonlinear system purely based on (non-derivative) data.

**Corollary 4.2.** *Let the assumptions of Theorem 4.1 hold and suppose additionally that the vector field  $f_c : \mathbb{R}^n \times \mathbb{R}^m \rightarrow \mathbb{R}^n$  with  $f_c(x, u) = f(x) + g(x)u$  corresponding to the nonlinear system (1) is continuous and locally Lipschitz in its first argument around the origin.*

*If there exist a matrix  $0 \prec P = P^\top \in \mathbb{R}^{N \times N}$ , matrices  $L \in \mathbb{R}^{m \times N}$ ,  $L_w \in \mathbb{R}^{m \times Nm}$ , a matrix  $0 \prec \Lambda = \Lambda^\top \in \mathbb{R}^{m \times m}$ , and scalars  $\nu > 0$ ,  $\tau > 0$  such that (17) and (18) hold, then there exists an amount of data  $d_0 \in \mathbb{N}$  such that for all  $d \geq d_0$  the controller*

$$\mu_s(x(t)) = \mu(x(k\Delta t)), \quad t \in [k\Delta t, (k+1)\Delta t), \quad k \geq 0 \quad (20)$$

*ensures safe operation by exponential stability of the continuous-time nonlinear system (1) for all initial conditions  $\hat{x} \in \mathcal{X}_{\text{SOR}} := \{x \in \mathbb{R}^n \mid \hat{\Phi}(x)^\top P^{-1} \hat{\Phi}(x) \leq 1\}$  with probability  $1 - \delta$ .*

*Proof.* This result can be proven building on [52, Thm. 2.27], which is elaborated in Appendix C.  $\square$

This corollary uses the stability certificates in Theorem 4.1, which are obtained for the sampled system (6), to infer the certificates also for the *true* continuous-time nonlinear system (1) using sampled feedback. Hence, the obtained closed-loop guarantees based on the introduced certified learning architecture hold for both sampled and continuous-time nonlinear systems.

## 5 Numerical experiments

To evaluate the proposed SafEDMD scheme, we perform a numerical study and compare our results to state-of-the-art Koopman-based control. All our simulations are conducted on an i7 notebook using Yalmip [53] with the semi-definite programming solver MOSEK [54] in Matlab. Full details on the system dynamics are provided in Appendix D.



**Nonlinear inverted pendulum** The inverted pendulum is a classical example for dynamical systems serving as a benchmark in nonlinear data-driven control, cf. [55, 56, 57, 58, 59, 60]). The dynamical system has two state variables  $x = (\theta, \dot{\theta})$ , i.e., the angular position  $\theta$  and the angular velocity  $\dot{\theta}$ , and one control input  $u$ . Further, we define the sets  $\mathbb{X} = [-2, 10]^2$  and  $\mathbb{U} = [-10, 10]$  whereof we uniformly sample  $d = 6000$  data points with sampling period  $\Delta t = 0.01$  s. More precisely, we consider imperfect measurements to illustrate the practical usability of our approach, i.e., we collect data  $\{x_j, \tilde{y}_j\}_{j=1}^d$  with  $\tilde{y}_j = y_j + \xi_j$ , where  $\xi_j$  is uniformly sampled from  $[-\bar{\xi}, \bar{\xi}]^2$  with  $\bar{\xi} = 0.01$ . We use the observables  $\hat{\Phi}(x) = [\theta \quad \dot{\theta} \quad \sin(\theta)]^\top$ , where the sine function is inspired by prior knowledge on the underlying nonlinear system. We use the proposed certified learning architecture SafEDMD in Algorithm 1 which yields a data-driven surrogate model (12) by linear regression. Moreover, we employ a learning error bound (15) with  $\delta = 0.05$  and  $c_x = c_u = 3 \times 10^{-4}$ , compare Corollary 3.2.

To illustrate the obtained certificates, we apply the robust controller design in Section 4 guaranteeing safe operation and closed-loop exponential stability of the nonlinear system. To apply the proposed scheme, we predefine the outer bound  $\Delta_\Phi$  on the SOR following the approach in [21, Procedure 8]. In particular, we first solve (17) for  $\tilde{Q}_z = -I$ ,  $\tilde{S}_z = 0$ , and arbitrary  $\tilde{R}_z > 0$  without considering the second linear matrix inequality (18). This leads to a matrix  $P$ , which relates the measured data and the chosen observables to maximize the SOR. Then, we incorporate this information in the actual controller design by defining  $\Delta_\Phi$  via  $Q_z = -\frac{P^{-1}}{\|P^{-1}\|_2}$ ,  $S_z = 0$ , and  $R_z > 0$ . Designing the nonlinear state-feedback controller (19) via Theorem 4.1 leads to the operation region depicted in Figure 3a, for which we can safely and reliably apply the control law  $\mu$  to the true nonlinear system. The closed-loop trajectories of the nonlinear system highlight that the system is indeed stabilized by our controller inside of the obtained region. We note that both Algorithm 1 as well as the controller design following Theorem 4.1 are solved in less than one second.

Next, we compare the learned surrogate model using SafEDMD to the state-of-the-art Koopman learning in the literature. While the literature on learning controllers for nonlinear systems is vast, we emphasize that other results are often achieved via completely different assumptions and provide different theoretical guarantees (if any). For example, [56] requires initial availability of a local linear quadratic regulator (LQR) as well as measurements of the vector field, i.e., state derivative data. Similarly, [61] requires state derivative measurements. On the contrary, our proposed control works for unknown continuous-time nonlinear systems using only discrete samples of the state requiring neither derivative data nor a pre-stabilizing controller. In the following, we compare the proposed approach (using a bilinear surrogate model) to an LQR based on a linear surrogate model, as considered, e.g., in [32, 10], see Appendix D for details. Based on this linear model, we design a linear LQR control law  $\mu_{\text{LQR}} = \hat{K}\hat{\Phi}(x)$  with matrix  $\hat{K} \in \mathbb{R}^{N \times N}$  defined in (48). We emphasize that the model obtained by EDMDC does not admit error certificates, compare [41, Sec. 5.3]. As a consequence, we observe in Figure 3a that  $\mu_{\text{LQR}}$  is not able to stabilize the origin of the underlying nonlinear system. Moreover, the obtained closed-loop behavior of the nonlinear system is highly sensitive to tuning parameters of the LQR. On the other hand, the proposed certified learning architecture SafEDMD with a bilinear lifted model and guaranteed learning error bounds leads to a stabilizing controller for the *unknown* nonlinear system (1) using the same data samples.

**Nonlinear system with Koopman invariant observables** Next, we consider a common nonlinear benchmark system which admits an invariant dictionary [32]. The system has a two-dimensional state and one input, for which we define the observable function  $\hat{\Phi}(x) = \left[ x_1 \quad x_2 \quad x_2 - \frac{\lambda}{\lambda - 2\rho} x_1^2 \right]^\top$ . For the data generation, we sample  $d = 100$  data points uniformly from the sets  $\mathbb{X} = [-1, 1]^2$  and  $\mathbb{U} = [-1, 1]$  with sampling rate  $\Delta t = 0.01$  s. Then, we learn a certified data-driven surrogate model via SafEDMD based on the generated data set and, particularly, without the need for derivative data. For a probabilistic tolerance  $\delta = 0.05$  and constants  $c_x = c_u = 5 \times 10^{-3}$  for the learning error bound (15), we apply the controller design in Theorem 4.1 with  $\Delta_\Phi$  defined by  $Q_z = -I$ ,  $S_z = 0$ , and  $R_z = 500$ . The obtained controller is guaranteed to ensure safe operation in the region  $\mathcal{X}_{\text{SOR}}$  shown in Figure 3b. Here,  $\mathcal{X}_{\text{SOR}}$  contains all  $x$  with  $\hat{\Phi}(x) \in \Delta_\Phi$  and, thus, adds no additional conservatism to the robust controller design. As before, both the learning and the controller design are completed in less than one second. In summary, also for this example, the controlled system under the proposed controller  $\mu$  operates reliably in the sense that it exponentially converges to the origin.

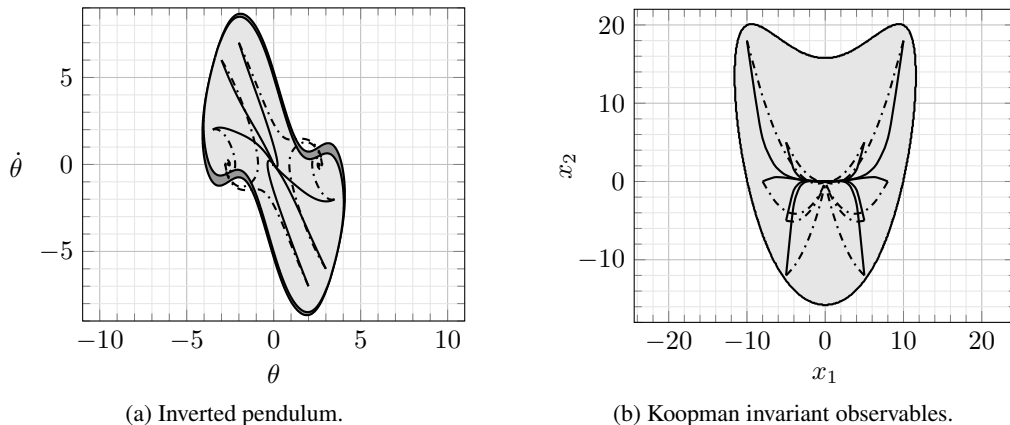


Figure 3: Region containing all  $x$  with  $\hat{\Phi}(x) \in \Delta_{\Phi}$  ( $\bullet$ ), SOR  $\mathcal{X}_{\text{SOR}}$  ( $\circ$ ), and closed-loop trajectories for the controllers  $\mu$  (—) and  $\mu_{\text{LQR}}$  (-·-·).

## 6 Conclusion

In conclusion, this paper introduced SafEDMD, a certified learning architecture tailored to data-driven control of nonlinear dynamical systems. Leveraging the analytical foundation of the Koopman operator, we showed that SafEDMD enables a rigorous and certified derivation of error bounds crucial for robust controller design. Unlike existing methods, the proposed architecture handles the Koopman operator directly via sampled data, eliminating the need for hard-to-obtain time-derivative data. SafEDMD offers a promising direction for the certified control of unknown nonlinear systems, demonstrating its superiority in scenarios where existing methods fail. This research not only tailors the capabilities of bilinear EDMD for control tasks but also establishes a new paradigm in the field of learning and control of data-driven surrogate models with rigorous stability certificates, addressing a critical aspect in safety-critical applications.

Interesting future work includes the integration of deep NNs as the observable function to exploit the superior robustness and scalability of EDMD-based approaches compared to state-of-the-art reinforcement learning methods (compare [62]).

## Acknowledgments and Disclosure of Funding

F. Allgöwer is thankful that this work was funded by the Deutsche Forschungsgemeinschaft (DFG, German Research Foundation) under Germany’s Excellence Strategy – EXC 2075 – 390740016 and within grant AL 316/15-1 – 468094890. K. Worthmann gratefully acknowledges funding by the German Research Foundation (DFG; project number 507037103). R. Strässer thanks the Graduate Academy of the SC SimTech for its support.

## References

- [1] Matthew Williams, Ioannis Kevrekidis, and Clarence Rowley. A data-driven approximation of the Koopman operator: Extending dynamic mode decomposition. *Journal of Nonlinear Science*, 25(6):1307–1346, 08 2015.
- [2] Omri Azencot, N. Benjamin Erichson, Vanessa Lin, and Michael Mahoney. Forecasting sequential data using consistent Koopman autoencoders. In *International Conference on Machine Learning*, pages 475–485. PMLR, 2020.
- [3] Tomer Golany, Kira Radinsky, Daniel Freedman, and Saar Minha. 12-lead ecg reconstruction via Koopman operators. In *International Conference on Machine Learning*, pages 3745–3754. PMLR, 2021.
- [4] Stefan Klus, Feliks Nüske, and Sebastian Peitz. Koopman analysis of quantum systems. *Journal of Physics A: Mathematical and Theoretical*, 55(31):314002, 2022.
- [5] Robin Strässer, Sebastian Schlor, and Frank Allgöwer. Decrypting nonlinearity: Koopman interpretation and analysis of cryptosystems. *arXiv:2311.12714*, 2023.

- [6] Igor Mezić. Analysis of fluid flows via spectral properties of the Koopman operator. *Annual review of fluid mechanics*, 45:357–378, 2013.
- [7] Vladimir Kostic, Pietro Novelli, Andreas Maurer, Carlo Ciliberto, Lorenzo Rosasco, and Massimiliano Pontil. Learning dynamical systems via Koopman operator regression in reproducing kernel Hilbert spaces. *Advances in Neural Information Processing Systems*, 35:4017–4031, 2022.
- [8] Friedrich Philipp, Manuel Schaller, Karl Worthmann, Sebastian Peitz, and Feliks Nüske. Error bounds for kernel-based approximations of the Koopman operator. *Applied and Computational Harmonic Analysis*, 2024.
- [9] Carl Folkestad, Yuxiao Chen, Aaron D. Ames, and Joel W. Burdick. Data-driven safety-critical control: Synthesizing control barrier functions with Koopman operators. *IEEE Control Systems Letters*, 5(6):2012–2017, 2020.
- [10] Milan Korda and Igor Mezić. Linear predictors for nonlinear dynamical systems: Koopman operator meets model predictive control. *Automatica*, 93:149–160, 2018.
- [11] Joshua L. Proctor, Steven L. Brunton, and J. Nathan Kutz. Generalizing Koopman theory to allow for inputs and control. *SIAM Journal on Applied Dynamical Systems*, 17(1):909–930, 2018.
- [12] Matthew O. Williams, Maziar S. Hemati, Scott T.M. Dawson, Ioannis G. Kevrekidis, and Clarence W. Rowley. Extending data-driven Koopman analysis to actuated systems. *IFAC-PapersOnLine*, 49(18):704–709, 2016.
- [13] Amit Surana. Koopman operator based observer synthesis for control-affine nonlinear systems. In *Proc. 55th IEEE Conference on Decision and Control (CDC)*, pages 6492–6499, 2016.
- [14] Petar Bevanda, Stefan Sosnowski, and Sandra Hirche. Koopman operator dynamical models: Learning, analysis and control. *Annual Reviews in Control*, 52:197–212, 2021.
- [15] Milan Korda and Igor Mezić. On convergence of extended dynamic mode decomposition to the Koopman operator. *Journal of Nonlinear Science*, 28(2):687–710, 2018.
- [16] Igor Mezić. On numerical approximations of the Koopman operator. *Mathematics*, 10(7):1180, 2022.
- [17] Christophe Zhang and Enrique Zuazua. A quantitative analysis of Koopman operator methods for system identification and predictions. *Comptes Rendus. Mécanique*, 351(S1):1–31, 2023.
- [18] Friedrich M Philipp, Manuel Schaller, Septimus Boshoff, Sebastian Peitz, Feliks Nüske, and Karl Worthmann. Variance representations and convergence rates for data-driven approximations of Koopman operators. *arXiv:2402.02494*, 2024.
- [19] Feliks Nüske, Sebastian Peitz, Friedrich Philipp, Manuel Schaller, and Karl Worthmann. Finite-data error bounds for Koopman-based prediction and control. *Journal of Nonlinear Science*, 33(1):14, 2023.
- [20] Lea Bold, Lars Grüne, Manuel Schaller, and Karl Worthmann. Practical asymptotic stability of data-driven model predictive control using extended DMD. *arXiv:2308.00296*, 2023.
- [21] Robin Strässer, Manuel Schaller, Karl Worthmann, Julian Berberich, and Frank Allgöwer. Koopman-based feedback design with stability guarantees. *arXiv:2312.01441*, 2023.
- [22] Bernard O. Koopman. Hamiltonian systems and transformation in Hilbert space. *Proc. of the National Academy of Sciences of the United States of America*, 17(5):315, 1931.
- [23] Pieter van Goor, Robert Mahony, Manuel Schaller, and Karl Worthmann. Reprojection methods for Koopman-based modelling and prediction. In *Proc. 62nd IEEE Conference on Decision and Control (CDC)*, pages 315–321, 2023.
- [24] Sebastian Peitz, Samuel E. Otto, and Clarence W. Rowley. Data-driven model predictive control using interpolated Koopman generators. *SIAM J. Applied Dynamical Systems*, 19(3):2162–2193, 2020.
- [25] Friedrich Philipp, Manuel Schaller, Karl Worthmann, Sebastian Peitz, and Feliks Nüske. Error analysis of kernel EDMD for prediction and control in the Koopman framework. *arXiv:2312.10460*, 2023.
- [26] Masih Haseli and Jorge Cortés. Generalizing dynamic mode decomposition: Balancing accuracy and expressiveness in Koopman approximations. *Automatica*, 153:111001, 2023.

- [27] Lu Shi and Konstantinos Karydis. Ac-demd: Analytical construction for dictionaries of lifting functions in Koopman operator-based nonlinear robotic systems. *IEEE Robotics and Automation Letters*, 7(2):906–913, 2021.
- [28] Enoch Yeung, Soumya Kundu, and Nathan Hodas. Learning deep neural network representations for Koopman operators of nonlinear dynamical systems. In *Proc. IEEE American Control Conference (ACC)*, pages 4832–4839, 2019.
- [29] Patricia Pauli, Anne Koch, Julian Berberich, Paul Kohler, and Frank Allgöwer. Training robust neural networks using Lipschitz bounds. *IEEE Control Systems Letters*, 6:121–126, 2021.
- [30] Samuel Otto, Sebastian Peitz, and Clarence Rowley. Learning bilinear models of actuated koopman generators from partially observed trajectories. *SIAM Journal on Applied Dynamical Systems*, 23(1):885–923, 2024.
- [31] Liam Llamazares-Elias, Samir Llamazares-Elias, Jonas Latz, and Stefan Klus. Data-driven approximation of Koopman operators and generators: Convergence rates and error bounds. *arXiv:2405.00539*, 2024.
- [32] Steven L. Brunton, Bingni W. Brunton, Joshua L. Proctor, and J. Nathan Kutz. Koopman invariant subspaces and finite linear representations of nonlinear dynamical systems for control. *PloS one*, 11(2):1–19, 2016.
- [33] Debdipta Goswami and Derek A. Paley. Global bilinearization and controllability of control-affine nonlinear systems: A Koopman spectral approach. In *Proc. 56th IEEE Conference on Decision and Control (CDC)*, pages 6107–6112, 2017.
- [34] Bowen Huang, Xu Ma, and Umesh Vaidya. Feedback stabilization using Koopman operator. In *Proc. 57th IEEE Conference on Decision and Control (CDC)*, pages 6434–6439, 2018.
- [35] Alexandre Mauroy, Aivar Sootla, and Igor Mezić. Koopman framework for global stability analysis. *The Koopman operator in Systems and Control*, pages 35–58, 2020.
- [36] Debdipta Goswami and Derek A. Paley. Global bilinearization and reachability analysis of control-affine nonlinear systems. *The Koopman Operator in Systems and Control*, pages 81–98, 2020.
- [37] Debdipta Goswami and Derek A. Paley. Bilinearization, reachability, and optimal control of control-affine nonlinear systems: A Koopman spectral approach. *IEEE Transactions on Automatic Control*, 67(6):2715–2728, 2021.
- [38] Jan C. Schulze, Danimir T. Doncevic, and Alexander Mitsos. Identification of MIMO Wiener-type Koopman models for data-driven model reduction using deep learning. *Computers & Chemical Engineering*, 161:107781, 2022.
- [39] Milan Korda and Igor Mezić. Optimal construction of Koopman eigenfunctions for prediction and control. *IEEE Transactions on Automatic Control*, 65(12):5114–5129, 2020.
- [40] Manuel Schaller, Karl Worthmann, Friedrich Philipp, Sebastian Peitz, and Feliks Nüske. Towards reliable data-based optimal and predictive control using extended DMD. *IFAC-PapersOnLine*, 56(1):169–174, 2023.
- [41] Lucian Cristian Iacob, Roland Tóth, and Maarten Schoukens. Koopman form of nonlinear systems with inputs. *Automatica*, 162:111525, 2024.
- [42] Rishikesh Yadav and Alexandre Mauroy. Approximation of the Koopman operator via bernstein polynomials. *arXiv:2403.02438*, 2024.
- [43] Frederik Köhne, Friedrich M. Philipp, Manuel Schaller, Anton Schiela, and Karl Worthmann.  $L^\infty$ -error bounds for approximations of the Koopman operator by kernel extended dynamic mode decomposition. *arXiv:2403.18809*, 2024.
- [44] Hassan K. Khalil. *Nonlinear systems*. Prentice-Hall, Upper Saddle River, NJ, third edition, 2002.
- [45] Stefan Klus, Andreas Bittracher, Ingmar Schuster, and Christof Schütte. A kernel-based approach to molecular conformation analysis. *The Journal of Chemical Physics*, 149(24), 2018.
- [46] Feliks Nüske and Stefan Klus. Efficient approximation of molecular kinetics using random Fourier features. *The Journal of Chemical Physics*, 159(7), 2023.
- [47] Lieven Vandenbergh and Stephen Boyd. Semidefinite programming. *SIAM review*, 38(1):49–95, 1996.

- [48] Etienne De Klerk. Exploiting special structure in semidefinite programming: A survey of theory and applications. *European Journal of Operational Research*, 201(1):1–10, 2010.
- [49] Dennis Gramlich, Tobias Holicki, Carsten W. Scherer, and Christian Ebenbauer. A structure exploiting sdp solver for robust controller synthesis. *IEEE Control Systems Letters*, 7:1831–1836, 2023.
- [50] Robin Strässer, Julian Berberich, and Frank Allgöwer. Robust data-driven control for nonlinear systems using the Koopman operator. *IFAC-PapersOnLine*, 56(2):2257–2262, 2023.
- [51] Robin Strässer, Julian Berberich, and Frank Allgöwer. Control of bilinear systems using gain-scheduling: Stability and performance guarantees. In *Proc. 62nd IEEE Conference on Decision and Control (CDC)*, pages 4674–4681, 2023.
- [52] Lars Grüne and Jürgen Pannek. *Nonlinear model predictive control*. Springer, 2017.
- [53] Johan Löfberg. YALMIP: A toolbox for modeling and optimization in MATLAB. In *Proc. IEEE International Conference on Robotics and Automation*, pages 284–289, 2004.
- [54] MOSEK ApS. *The MOSEK optimization toolbox for MATLAB manual. Version 9.3.21*, 2022.
- [55] Tom Bertalan, Felix Dietrich, Igor Mezić, and Ioannis G. Kevrekidis. On learning Hamiltonian systems from data. *Chaos: An Interdisciplinary Journal of Nonlinear Science*, 29(12), 2019.
- [56] Ya-Chien Chang, Nima Roohi, and Sicun Gao. Neural Lyapunov control. *Advances in neural information processing systems*, 32, 2019.
- [57] Robin Strässer, Julian Berberich, and Frank Allgöwer. Data-driven control of nonlinear systems: Beyond polynomial dynamics. In *Proc. 60th IEEE Conference on Decision and Control (CDC)*, pages 4344–4351, 2021.
- [58] Chris Verhoeck, Hossam S. Abbas, and Roland Tóth. Direct data-driven LPV control of nonlinear systems: An experimental result. *IFAC-PapersOnLine*, 56(2):2263–2268, 2023.
- [59] Madhur Tiwari, George Nehma, and Bethany Lusch. Computationally efficient data-driven discovery and linear representation of nonlinear systems for control. *IEEE Control Systems Letters*, 7:3373–3378, 2023.
- [60] Tim Martin, Thomas B. Schön, and Frank Allgöwer. Guarantees for data-driven control of nonlinear systems using semidefinite programming: A survey. *Annual Reviews in Control*, page 100911, 2023.
- [61] Jingdong Zhang, Qunxi Zhu, and Wei Lin. Neural stochastic control. *Advances in Neural Information Processing Systems*, 35:9098–9110, 2022.
- [62] Minghao Han, Jacob Euler-Rolle, and Robert K. Katzschmann. DeSKO: Stability-assured robust control with a deep stochastic Koopman operator. In *International Conference on Learning Representations*. ICLR, 2022.
- [63] Carsten W. Scherer and Siep Weiland. Linear matrix inequalities in control. *Lecture Notes, Dutch Institute for Systems and Control, Delft, The Netherlands*, 3(2), 2000.
- [64] Stephen P. Boyd and Lieven Vandenbergh. *Convex Optimization*. Cambridge University Press, 2004.

## A Proof of Theorem 3.1

In this section, we prove Theorem 3.1, which builds the foundation of SafEDMD: A novel certified learning architecture for data-driven control of nonlinear dynamical systems. To this end, we first introduce a finite-dimensional bilinear representation for the projected Koopman operator in Lemma A.1 before defining a data-driven surrogate model for the bilinear representation in Lemma A.3. Then, Theorem 3.1 results as a direct consequence of the preliminary lemmas.

### A.1 Bilinear representation for the Koopman operator

The proposed certified learning architecture relies on a bilinear representation of the projected Koopman operator  $P_{\mathbb{V}}\mathcal{K}_{\Delta t}^u|_{\mathbb{V}}$ . For the setting in this paper and for a fixed control value  $u \in \mathbb{U}$ ,  $(\mathcal{K}_t^u)_{t \geq 0}$  is a strongly-continuous semigroup of bounded linear operators, i.e., we can define its infinitesimal generator  $\mathcal{L}^u$  via

$$\mathcal{L}^u \varphi := \lim_{t \searrow 0} \frac{\mathcal{K}_t^u \varphi - \varphi}{t} \quad \forall \varphi \in D(\mathcal{L}^u),$$

where the domain  $D(\mathcal{L}^u)$  consists of all  $L^2$ -functions for which the above limit exists. By definition of this generator, the propagated observable satisfies  $\dot{\varphi}(x) = \mathcal{L}^u \varphi(x)$ . A key structural property of the Koopman generator, also called Liouville operator, is that control affinity is preserved [12, 13], i.e., for  $u \in \mathbb{R}^m$  we have

$$\mathcal{L}^u = \mathcal{L}^0 + \sum_{i=1}^m u_i (\mathcal{L}^{e_i} - \mathcal{L}^0), \quad (21)$$

where  $\mathcal{L}^0$  and  $\mathcal{L}^{e_i}$ ,  $i \in [m]$ , are the generators of the Koopman semigroups corresponding to the constant control functions  $u \equiv 0$  and  $u \equiv e_i$  with the unit vector  $e_i$ ,  $i \in [m]$ , respectively. Hence, the Koopman generator acting on the vector-valued observable function  $\Phi$  in (4) has a specific structure due to the included constant observable  $\phi_0 \equiv 1$ . In particular, we obtain

$$\mathcal{L}^u = \begin{bmatrix} 0 & 0 \\ \mathcal{L}_{21}^u & \mathcal{L}_{22}^u \end{bmatrix} \quad \text{using (21) with } \mathcal{L}^0 = \begin{bmatrix} 0 & 0 \\ 0 & \mathcal{L}_{22}^0 \end{bmatrix} \quad \text{and } \mathcal{L}^{e_i} = \begin{bmatrix} 0 & 0 \\ \mathcal{L}_{21}^{e_i} & \mathcal{L}_{22}^{e_i} \end{bmatrix}, \quad (22)$$

$i \in [m]$ . The structure of the matrices in (22) corresponds to the structure of the Koopman operator (8) in the proposed learning architecture. We stress that in this work, the Koopman generator is only used in the proofs. In particular, our learning scheme directly approximates the Koopman operator by means of trajectory samples. This avoids the use of (typically extremely-noisy) derivative data necessary to approximate the Koopman generator in view of  $\mathcal{L}^u \Phi(x) = \langle \nabla \Phi(x), \dot{x}(t) \rangle = \langle \nabla \Phi(x), f(x(t)) + \sum_{i=1}^m g_i(x(t)) u_i(t) \rangle$ . In conclusion, this makes our learning scheme data-efficient and robust in comparison to competing methods, for which similar error estimates exist [20, 21] and whose derivations have inspired the following lemma and its proof.

In the following, we leverage the control affine structure (21) of the generator  $\mathcal{L}^u$  to study the Koopman operator given by  $P_{\mathbb{V}}\mathcal{K}_{\Delta t}^u|_{\mathbb{V}} = \exp(\Delta t P_{\mathbb{V}} \mathcal{L}^u|_{\mathbb{V}})$ . To this end, we recall (3) and define

$$P_{\mathbb{V}}\mathcal{K}_{\Delta t}^u|_{\mathbb{V}} = P_{\mathbb{V}}\mathcal{K}_{\Delta t}^0|_{\mathbb{V}} + \sum_{i=1}^m u_i (P_{\mathbb{V}}\mathcal{K}_{\Delta t}^{e_i}|_{\mathbb{V}} - P_{\mathbb{V}}\mathcal{K}_{\Delta t}^0|_{\mathbb{V}}) + h(\Delta t)$$

with

$$h(\Delta t) := P_{\mathbb{V}}\mathcal{K}_{\Delta t}^u|_{\mathbb{V}} - \left[ P_{\mathbb{V}}\mathcal{K}_{\Delta t}^0|_{\mathbb{V}} + \sum_{i=1}^m u_i (P_{\mathbb{V}}\mathcal{K}_{\Delta t}^{e_i}|_{\mathbb{V}} - P_{\mathbb{V}}\mathcal{K}_{\Delta t}^0|_{\mathbb{V}}) \right]. \quad (23)$$

Further, we define  $\xi(x, u) := h(\Delta t)\Phi(x)$  to obtain

$$(P_{\mathbb{V}}\mathcal{K}_{\Delta t}^u|_{\mathbb{V}})\Phi(x) = (P_{\mathbb{V}}\mathcal{K}_{\Delta t}^0|_{\mathbb{V}})\Phi(x) + \sum_{i=1}^m u_i (P_{\mathbb{V}}\mathcal{K}_{\Delta t}^{e_i}|_{\mathbb{V}} - P_{\mathbb{V}}\mathcal{K}_{\Delta t}^0|_{\mathbb{V}})\Phi(x) + \xi(x, u).$$

The following lemma formulates a proportional bound on the approximation error  $\xi$  of the bilinear representation of the Koopman operator.

**Lemma A.1.** *The approximation error  $\xi$  due to the bilinear representation of the projected Koopman operator  $P_{\mathbb{V}}\mathcal{K}_{\Delta t}^u|_{\mathbb{V}}$  satisfies the proportional bound*

$$\|\xi(x, u)\| \leq \Delta t^2 (c_1 \|\Phi(x) - \Phi(0)\| + \sqrt{m} c_2 \|u\|), \quad (24)$$

where  $c_1, c_2 \in \mathbb{R}_+$  are defined in (27) and (29).

*Proof.* Recall the definition of  $\xi(x, u) = h(\Delta t)\Phi(x)$  with  $h(\Delta t)$  defined in (23). Then, we bound the norm of  $\xi(x, u)$  by

$$\begin{aligned} \|\xi(x, u)\| &= \|h(\Delta t)(\Phi(x) - \Phi(0) + \Phi(0))\| \leq \|h(\Delta t)(\Phi(x) - \Phi(0))\| + \|h(\Delta t)\Phi(0)\| \\ &\leq \|h(\Delta t)\| \|\Phi(x) - \Phi(0)\| + \|h(\Delta t)\Phi(0)\|. \end{aligned} \quad (25)$$

To estimate the first term in (25), we substitute  $P_{\mathbb{V}}\mathcal{K}_{\Delta t}^u|_{\mathbb{V}} = e^{\Delta t P_{\mathbb{V}}\mathcal{L}^u|_{\mathbb{V}}}$ ,  $P_{\mathbb{V}}\mathcal{K}_{\Delta t}^0|_{\mathbb{V}} = e^{\Delta t P_{\mathbb{V}}\mathcal{L}^0|_{\mathbb{V}}}$ , and  $P_{\mathbb{V}}\mathcal{K}_{\Delta t}^{e_i}|_{\mathbb{V}} = e^{\Delta t P_{\mathbb{V}}\mathcal{L}^{e_i}|_{\mathbb{V}}}$ ,  $i \in [m]$ , to obtain

$$\begin{aligned} h(\Delta t) &= e^{\Delta t (P_{\mathbb{V}}\mathcal{L}^0|_{\mathbb{V}} + \sum_{i=1}^m u_i (P_{\mathbb{V}}\mathcal{L}^{e_i}|_{\mathbb{V}} - P_{\mathbb{V}}\mathcal{L}^0|_{\mathbb{V}}))} \\ &\quad - \left( e^{\Delta t P_{\mathbb{V}}\mathcal{L}^0|_{\mathbb{V}}} + \sum_{i=1}^m u_i \left( e^{\Delta t P_{\mathbb{V}}\mathcal{L}^{e_i}|_{\mathbb{V}}} - e^{\Delta t P_{\mathbb{V}}\mathcal{L}^0|_{\mathbb{V}}} \right) \right). \end{aligned} \quad (26)$$

Then, the Taylor series expansion for  $h(\Delta t)$  at  $\Delta t = 0$  yields, in view of  $h(0) = 0$  and  $\frac{\partial h}{\partial \Delta t}(0) = 0$ ,

$$\begin{aligned} h(\Delta t) &= h(0) + \Delta t \frac{\partial h}{\partial \Delta t}(0) + \frac{\Delta t^2}{2} \frac{\partial^2 h}{\partial \Delta t^2}(\tau) \\ &= \frac{\Delta t^2}{2} \left[ e^{\tau (P_{\mathbb{V}}\mathcal{L}^0|_{\mathbb{V}} + \sum_{i=1}^m u_i (P_{\mathbb{V}}\mathcal{L}^{e_i}|_{\mathbb{V}} - P_{\mathbb{V}}\mathcal{L}^0|_{\mathbb{V}}))} \left( P_{\mathbb{V}}\mathcal{L}^0|_{\mathbb{V}} + \sum_{i=1}^m u_i (P_{\mathbb{V}}\mathcal{L}^{e_i}|_{\mathbb{V}} - P_{\mathbb{V}}\mathcal{L}^0|_{\mathbb{V}}) \right)^2 \right. \\ &\quad \left. - \left( e^{\tau P_{\mathbb{V}}\mathcal{L}^0|_{\mathbb{V}}} (P_{\mathbb{V}}\mathcal{L}^0|_{\mathbb{V}})^2 + \sum_{i=1}^m u_i \left( e^{\tau P_{\mathbb{V}}\mathcal{L}^{e_i}|_{\mathbb{V}}} (P_{\mathbb{V}}\mathcal{L}^{e_i}|_{\mathbb{V}})^2 - e^{\tau P_{\mathbb{V}}\mathcal{L}^0|_{\mathbb{V}}} (P_{\mathbb{V}}\mathcal{L}^0|_{\mathbb{V}})^2 \right) \right) \right] \end{aligned}$$

for some  $\tau \in [0, \Delta t]$ . Hence, we can derive the following estimate using the triangle inequality

$$\begin{aligned} \frac{2\|h(\Delta t)\|}{\Delta t^2} &\leq \left\| e^{\tau (P_{\mathbb{V}}\mathcal{L}^0|_{\mathbb{V}} + \sum_{i=1}^m u_i (P_{\mathbb{V}}\mathcal{L}^{e_i}|_{\mathbb{V}} - P_{\mathbb{V}}\mathcal{L}^0|_{\mathbb{V}}))} \right\| \left\| P_{\mathbb{V}}\mathcal{L}^0|_{\mathbb{V}} + \sum_{i=1}^m u_i (P_{\mathbb{V}}\mathcal{L}^{e_i}|_{\mathbb{V}} - P_{\mathbb{V}}\mathcal{L}^0|_{\mathbb{V}}) \right\|^2 \\ &\quad + \left\| e^{\tau P_{\mathbb{V}}\mathcal{L}^0|_{\mathbb{V}}} (P_{\mathbb{V}}\mathcal{L}^0|_{\mathbb{V}})^2 + \sum_{i=1}^m u_i \left( e^{\tau P_{\mathbb{V}}\mathcal{L}^{e_i}|_{\mathbb{V}}} (P_{\mathbb{V}}\mathcal{L}^{e_i}|_{\mathbb{V}})^2 - e^{\tau P_{\mathbb{V}}\mathcal{L}^0|_{\mathbb{V}}} (P_{\mathbb{V}}\mathcal{L}^0|_{\mathbb{V}})^2 \right) \right\| \\ &\leq e^{\Delta t (\hat{u} \|P_{\mathbb{V}}\mathcal{L}^0|_{\mathbb{V}}\| + \sum_{i=1}^m |u_i| \|P_{\mathbb{V}}\mathcal{L}^{e_i}|_{\mathbb{V}}\|)} \left( \hat{u} \|P_{\mathbb{V}}\mathcal{L}^0|_{\mathbb{V}}\| + \sum_{i=1}^m |u_i| \|P_{\mathbb{V}}\mathcal{L}^{e_i}|_{\mathbb{V}}\| \right)^2 \\ &\quad + \hat{u} e^{\Delta t \|P_{\mathbb{V}}\mathcal{L}^0|_{\mathbb{V}}\|} \|P_{\mathbb{V}}\mathcal{L}^0|_{\mathbb{V}}\|^2 + \sum_{i=1}^m |u_i| e^{\Delta t \|P_{\mathbb{V}}\mathcal{L}^{e_i}|_{\mathbb{V}}\|} \|P_{\mathbb{V}}\mathcal{L}^{e_i}|_{\mathbb{V}}\|^2 =: 2c_1 \end{aligned} \quad (27)$$

with  $\hat{u} := \max_{u \in \mathbb{U}} |1 - \sum_{i=1}^m u_i|$ . The constant  $c_1$  is finite for a compact set  $\mathbb{U}$  of control actions. Hence, we have  $\|h(\Delta t)\| \leq \Delta t^2 c_1 < \infty$ . The terms  $\|P_{\mathbb{V}}\mathcal{L}^{\bar{u}}|_{\mathbb{V}}\|$  with  $\bar{u} \in \{0, e_1, \dots, e_m\}$  can be further bounded in terms of the system dynamics. To see this, we plug in the definition of the operator norm of  $P_{\mathbb{V}}\mathcal{L}|_{\mathbb{V}}$  as a mapping from  $\mathbb{V}$  to  $\mathbb{V}$ , where we endow the finite-dimensional subspace  $\mathbb{V}$  of  $L^2(X)$  with the  $L^2$ -norm. W.l.o.g. the basis elements are scaled such that  $\|\phi_\ell\|_{L^2(X)} = 1$ ,  $\ell \in [0 : N]$ , holds. Then, we obtain

$$\begin{aligned} \|P_{\mathbb{V}}\mathcal{L}^0|_{\mathbb{V}}\| &= \sup_{\substack{\varphi \in \mathbb{V}, \\ \|\varphi\|_{L^2} = 1}} \|\nabla \varphi(\cdot)^\top f(\cdot)\|_{L^2(X)} = \sup_{\ell \in [0 : N]} \|\nabla \phi_\ell(\cdot)^\top f(\cdot)\|_{L^2(X)} \\ &\leq \sup_{\ell \in [0 : N]} \|\nabla \phi_\ell\|_{L^2(X)} \|f\|_{L^2(X)} \end{aligned} \quad (28)$$

and, analogously,  $\|P_{\mathbb{V}}\mathcal{L}^{e_i}|_{\mathbb{V}}\| \leq \sup_{\ell \in [0 : N]} \|\nabla \phi_\ell\|_{L^2(X)} \|f + g_i\|_{L^2(X)}$ ,  $i \in [m]$ .

For an estimate on the second term in (25), we again use the Taylor expansion (26), the triangle inequality, and the notation and arguments used to derive Inequality (28) to get the estimate

$$\begin{aligned}
\frac{2\|h(\Delta t)\Phi(0)\|}{\Delta t^2} &\leq \underbrace{\left( e^{\Delta t(\hat{u}\|P_V\mathcal{L}^0|_V\| + \sum_{i=1}^m |u_i|\|P_V\mathcal{L}^{e_i}|_V\|)} \left( \hat{u}\|P_V\mathcal{L}^0|_V\| + \sum_{i=1}^m |u_i|\|P_V\mathcal{L}^{e_i}|_V\| \right) \right)}_{=:\tilde{c}} \\
&\quad \cdot \left\| \left( 1 - \sum_{i=1}^m u_i \right) \underbrace{(P_V\mathcal{L}^0|_V)\Phi(0)}_{=0} + \sum_{i=1}^m u_i \underbrace{(P_V\mathcal{L}^{e_i}|_V)\Phi(0)}_{=(P_V\mathcal{L}^{e_i}|_V)_{21}} \right\| \\
&\quad + \left\| \left( \left( 1 - \sum_{i=1}^m u_i \right) e^{\tau P_V\mathcal{L}^0|_V} P_V\mathcal{L}^0|_V \right) \underbrace{(P_V\mathcal{L}^0|_V)\Phi(0)}_{=0} \right\| \\
&\quad + \left\| \sum_{i=1}^m u_i e^{\tau P_V\mathcal{L}^{e_i}|_V} (P_V\mathcal{L}^{e_i}|_V)^2 \Phi(0) \right\| \\
&\leq \tilde{c} \left[ \|(P_V\mathcal{L}^{e_1}|_V)_{21} \cdots (P_V\mathcal{L}^{e_m}|_V)_{21}\| \|u\| \right. \\
&\quad \left. + \left\| [e^{\tau P_V\mathcal{L}^{e_1}|_V} (P_V\mathcal{L}^{e_1}|_V)^2 \Phi(0) \cdots e^{\tau P_V\mathcal{L}^{e_m}|_V} (P_V\mathcal{L}^{e_m}|_V)^2 \Phi(0)] \right\| \|u\| \right] \\
&\leq \tilde{c} \sqrt{\sum_{i=1}^m \|(P_V\mathcal{L}^{e_i}|_V)_{21}\|^2} \|u\| \\
&\quad + \sqrt{\sum_{i=1}^m (e^{\Delta t\|P_V\mathcal{L}^{e_i}|_V\|} \|(P_V\mathcal{L}^{e_i}|_V)_{22}\| \|(P_V\mathcal{L}^{e_i}|_V)_{21}\|)^2} \|u\| \\
&\leq \tilde{c}\sqrt{m}\|\mathcal{L}_{21}^*\| \|u\| \sqrt{m}e^{\Delta t\|\mathcal{L}^*\|} \|\mathcal{L}_{22}^*\| \|\mathcal{L}_{21}^*\| \|u\| =: 2\sqrt{m}c_2\|u\| \tag{29}
\end{aligned}$$

using  $(P_V\mathcal{L}^{e_i}|_V)^2\Phi(0) = (P_V\mathcal{L}^{e_i}|_V)_{22}(P_V\mathcal{L}^{e_i}|_V)_{21}\Phi(0)$ , the notations  $\|\mathcal{L}_{21}^*\| := \max_{i \in [m]} \|(P_V\mathcal{L}^{e_i}|_V)_{21}\|$ ,  $\|\mathcal{L}_{22}^*\| := \max_{i \in [m]} \|(P_V\mathcal{L}^{e_i}|_V)_{22}\|$ , and  $\|\mathcal{L}^*\| := \max_{i \in [m]} \|P_V\mathcal{L}^{e_i}|_V\|$ , respectively. Thus, we have  $\|h(\Delta t)\Phi(0)\| \leq \Delta t^2 \sqrt{m}c_2\|u\|$ .

Hence, combining the two derived estimates (27) and (29) yields  $\|\xi(x, u)\| \leq \Delta t^2(c_1\|\Phi(x) - \Phi(0)\| + \sqrt{m}c_2\|u\|)$ , i.e., the desired inequality.  $\square$

Here, we emphasize that the constants  $c_1, c_2$  in Lemma A.1 can be computed if, e.g., a bound on the  $L^2$ -norm of the system dynamics is given.

## A.2 Data-driven surrogate of the bilinear representation of the Koopman operator

Next, we approximate the bilinear representation of the projected Koopman operator by its respective data-driven estimates. To this end, we consider the data-driven surrogate model

$$\begin{aligned}
(P_V\mathcal{K}_{\Delta t}^u|_V)\Phi(x_k) &= \mathcal{K}_{\Delta t,d}^u\Phi(x_k) + \xi(x_k, u_k) + \eta(x_k, u_k) \\
&= \mathcal{K}_{\Delta t,d}^0\Phi(x_k) + \sum_{i=1}^m u_{k,i}(\mathcal{K}_{\Delta t,d}^{e_i} - \mathcal{K}_{\Delta t,d}^0)\Phi(x_k) + \xi(x_k, u_k) + \eta(x_k, u_k)
\end{aligned}$$



corresponding to (12), where

$$\begin{aligned}
\eta(x, u) &= \left( (P_{\mathbb{V}}\mathcal{K}_{\Delta t}^0|_{\mathbb{V}})\Phi(x) + \sum_{i=1}^m u_i (P_{\mathbb{V}}\mathcal{K}_{\Delta t}^{e_i}|_{\mathbb{V}} - P_{\mathbb{V}}\mathcal{K}_{\Delta t}^0|_{\mathbb{V}})\Phi(x) \right) \\
&\quad - \left( \mathcal{K}_{\Delta t, d}^0\Phi(x) + \sum_{i=1}^m u_i (\mathcal{K}_{\Delta t, d}^{e_i} - \mathcal{K}_{\Delta t, d}^0)\Phi(x) \right) \\
&= \left( (P_{\mathbb{V}}\mathcal{K}_{\Delta t}^0|_{\mathbb{V}} - \mathcal{K}_{\Delta t, d}^0) + \sum_{i=1}^m u_i (P_{\mathbb{V}}\mathcal{K}_{\Delta t}^{e_i}|_{\mathbb{V}} - \mathcal{K}_{\Delta t, d}^{e_i}) \right. \\
&\quad \left. + \sum_{i=1}^m u_i (P_{\mathbb{V}}\mathcal{K}_{\Delta t, d}^0|_{\mathbb{V}} - \mathcal{K}_{\Delta t}^0) \right) \Phi(x) \tag{30}
\end{aligned}$$

describes the estimation error due to the learning via sampled data. Before stating a bound on  $\eta$ , we first introduce the following proposition from the literature.

**Proposition A.2** ([19, Thm. 14]). *Suppose that the data samples are i.i.d. Further, let an error bound  $c_\eta > 0$  and a probabilistic tolerance  $\delta \in (0, 1)$  be given. Then, there is an amount of data  $d_0^{\bar{u}} = \mathcal{O}(1/\delta c_\eta^2)$  such that for all  $d \geq d_0^{\bar{u}}$  we have the error bound*

$$\|P_{\mathbb{V}}\mathcal{K}_{\Delta t}^{\bar{u}}|_{\mathbb{V}} - \mathcal{K}_{\Delta t, d}^{\bar{u}}\| \leq c_\eta \tag{31}$$

for a fixed control input  $\bar{u}$  with probability  $1 - \delta$ .

Now, we show that the sampling error  $\eta$  in (30) satisfies the following proportional bound, where we exploit that Proposition A.2 can be applied for any  $\bar{u} \in \{0, e_1, \dots, e_m\}$ .

**Lemma A.3.** *Suppose that the data samples are i.i.d. Further, let an error bound  $c_\eta > 0$  and a probabilistic tolerance  $\delta \in (0, 1)$  be given. Then, there is an amount of data  $d_0 = \mathcal{O}(1/\delta c_\eta^2)$  such that for all  $d \geq d_0$  the approximation error  $\eta$  due to sampling of the Koopman operators  $\mathcal{K}_{\Delta t, d}^{\bar{u}}$ ,  $\bar{u} \in \{0, e_1, \dots, e_m\}$ , based on the data satisfies the proportional bound*

$$\|\eta(x, u)\| \leq c_3 c_\eta \|\Phi(x) - \Phi(0)\| + \sqrt{m} c_\eta \|u\| \tag{32}$$

with probability  $1 - \delta$ , where  $c_3 \in \mathbb{R}_+$  is defined in (33).

*Proof.* First, we apply Proposition A.2 for all  $\bar{u} \in \{0, e_1, \dots, e_m\}$  and the given error bound  $c_\eta$  and probabilistic tolerance  $\delta$ . This results in a necessary amount of data  $d_0^{\bar{u}} \in \mathbb{N}$  for each fixed control input  $\bar{u}$  such that the error bound (31) holds. We define the maximum of those necessary data lengths as  $d_0 = \max\{d_0^0, d_0^{e_1}, \dots, d_0^{e_m}\}$ . This ensures that the bound (31) holds for all data-driven estimates  $\mathcal{K}_{\Delta t, d}^{\bar{u}}$  of the Koopman operator, where  $\bar{u} \in \{0, e_1, \dots, e_m\}$ . Then, we recall the definition of the sampling error  $\eta$  in (30) and leverage  $\Phi(x) = \Phi(x) - \Phi(0) + \Phi(0)$  to obtain with  $\hat{u} := \max_{u \in \mathbb{U}} |1 - \sum_{i=1}^m u_i|$

$$\begin{aligned}
\|\eta(x, u)\| &\leq \hat{u} \|(P_{\mathbb{V}}\mathcal{K}_{\Delta t}^0|_{\mathbb{V}} - \mathcal{K}_{\Delta t, d}^0)(\Phi(x) - \Phi(0) + \Phi(0))\| \\
&\quad + \sum_{i=1}^m |u_i| \|(P_{\mathbb{V}}\mathcal{K}_{\Delta t}^{e_i}|_{\mathbb{V}} - \mathcal{K}_{\Delta t, d}^{e_i})(\Phi(x) - \Phi(0) + \Phi(0))\| \\
&\leq \left( \hat{u} \|P_{\mathbb{V}}\mathcal{K}_{\Delta t}^0|_{\mathbb{V}} - \mathcal{K}_{\Delta t, d}^0\| + \sum_{i=1}^m |u_i| \|P_{\mathbb{V}}\mathcal{K}_{\Delta t}^{e_i}|_{\mathbb{V}} - \mathcal{K}_{\Delta t, d}^{e_i}\| \right) \|\Phi(x) - \Phi(0)\| \\
&\quad + \hat{u} \|(P_{\mathbb{V}}\mathcal{K}_{\Delta t}^0|_{\mathbb{V}} - \mathcal{K}_{\Delta t, d}^0)\Phi(0)\| \\
&\quad + \|[ (P_{\mathbb{V}}\mathcal{K}_{\Delta t}^{e_1}|_{\mathbb{V}})_{21} - (\mathcal{K}_{\Delta t, d}^{e_1})_{21} \ \cdots \ (P_{\mathbb{V}}\mathcal{K}_{\Delta t}^{e_m}|_{\mathbb{V}})_{21} - (\mathcal{K}_{\Delta t, d}^{e_m})_{21} ]\| \|u\|.
\end{aligned}$$

Next, we exploit  $(P_{\mathbb{V}}\mathcal{K}_{\Delta t}^0|_{\mathbb{V}} - \mathcal{K}_{\Delta t, d}^0)\Phi(0) = 0$  due to the structure of the Koopman operator in (8) and its data-driven approximate in (9),  $\|P_{\mathbb{V}}\mathcal{K}_{\Delta t}^{\bar{u}}|_{\mathbb{V}} - \mathcal{K}_{\Delta t, d}^{\bar{u}}\| \leq c_\eta$  for  $\bar{u} \in \{0, e_1, \dots, e_m\}$  according to (31), and

$$\begin{aligned}
&\|[ (P_{\mathbb{V}}\mathcal{K}_{\Delta t}^{e_1}|_{\mathbb{V}})_{21} - (\mathcal{K}_{\Delta t, d}^{e_1})_{21} \ \cdots \ (P_{\mathbb{V}}\mathcal{K}_{\Delta t}^{e_m}|_{\mathbb{V}})_{21} - (\mathcal{K}_{\Delta t, d}^{e_m})_{21} ]\| \\
&\leq \sqrt{\sum_{i=1}^m \|(P_{\mathbb{V}}\mathcal{K}_{\Delta t}^{e_i}|_{\mathbb{V}})_{21} - (\mathcal{K}_{\Delta t, d}^{e_i})_{21}\|^2} \leq \sqrt{\sum_{i=1}^m \|P_{\mathbb{V}}\mathcal{K}_{\Delta t}^{e_i}|_{\mathbb{V}} - \mathcal{K}_{\Delta t, d}^{e_i}\|^2},
\end{aligned}$$

which results in (32) with

$$c_3 = 1 + 2 \max_{u \in \mathbb{U}} \|u\|_1. \quad (33)$$

This completes the proof.  $\square$

Again, we emphasize that the constant  $c_3$  in Lemma A.3 can be evaluated for a given set  $\mathbb{U}$ .

Now we can prove Theorem 3.1.

*Proof (Theorem 3.1).* This is a direct consequence of Lemma A.1 and Lemma A.3. We observe  $(P_{\mathbb{V}} \mathcal{K}_{\Delta t}^u|_{\mathbb{V}} - \mathcal{K}_{\Delta t, d}^u) \Phi(x) = \xi(x, u) + \eta(x, u)$  and use the estimates in (24) and (32) to deduce

$$\begin{aligned} \|(P_{\mathbb{V}} \mathcal{K}_{\Delta t}^u|_{\mathbb{V}} - \mathcal{K}_{\Delta t, d}^u) \Phi(x)\| &\leq \|\xi(x, u)\| + \|\eta(x, u)\| \\ &\leq (\Delta t^2 c_1 + c_3) \|\Phi(x) - \Phi(0)\| + \sqrt{m}(\Delta t^2 c_2 + c_\eta) \|u\|. \end{aligned}$$

Then, defining

$$\bar{c}_x = \Delta t^2 c_1 + c_3 c_\eta \quad \text{and} \quad \bar{c}_u = \sqrt{m}(\Delta t^2 c_2 + c_\eta). \quad (34)$$

results in (13). In view of Lemma A.3, and for any probabilistic tolerance  $\delta \in (0, 1)$ , the constant  $c_\eta$  is of order  $c_\eta = \mathcal{O}(1/\sqrt{\delta d_0})$  which implies the claim  $\bar{c}_x, \bar{c}_u = \mathcal{O}(1/\sqrt{\delta d_0} + \Delta t^2)$ .  $\square$

## B Proof of Theorem 4.1

In the following, we prove Theorem 4.1 guaranteeing safe operation by exponential stability of the sampled nonlinear system (6) with the feedback control law (19). To this end, we first observe that the inclusion of the constant observable  $\phi_0 \equiv 1$  and the thereof resulting structure of the Koopman operator (8) and its data-driven approximates (9) allows the simplification of the data-driven surrogate model

$$\begin{aligned} \Phi(x_{k+1}) &= \mathcal{K}_{\Delta t, d}^u \Phi(x) + (\mathcal{K}_{\Delta t}^u - \mathcal{K}_{\Delta t, d}^u) \Phi(x) \\ &= \mathcal{K}_{\Delta t, d}^0 \Phi(x_k) + \sum_{i=1}^m (u_k)_i (\mathcal{K}_{\Delta t, d}^{e_i} - \mathcal{K}_{\Delta t, d}^0) \Phi(x_k) + \zeta(x_k, u_k) \end{aligned}$$

with  $\zeta := (\mathcal{K}_{\Delta t, d}^u - \mathcal{K}_{\Delta t, d}^0) \Phi(x)$ . In particular, we observe that the first element of the learning error  $\zeta$  is zero and, thus,  $\|\zeta(x, u)\| = \|\hat{\zeta}(x, u)\|$  with  $\hat{\zeta}(x, u) := [0_{N \times 1} \quad I_N] \zeta(x, u)$ . Further, we exploit the structure in (8), (9) to deduce the lifted system representation

$$\begin{aligned} \hat{\Phi}(x_{k+1}) &= A \hat{\Phi}(x_k) + B_0 u_k + \sum_{i=1}^m (u_k)_i (\hat{B}_i - A) \hat{\Phi}(x_k) + \hat{\zeta}(x, u) \\ &= A \hat{\Phi}(x_k) + B_0 u_k + \tilde{B}(u_k \otimes \hat{\Phi}(x_k)) + \hat{\zeta}(x, u) \end{aligned} \quad (35)$$

with  $B_0 = [B_{0,1} \quad \dots \quad B_{0,m}]$  and  $\tilde{B} = [\hat{B}_1 - A \quad \dots \quad \hat{B}_m - A]$ . Here, we use the reduced observable function  $\hat{\Phi}(x) = [0_{N \times 1} \quad I_N] \Phi(x)$ , where we removed the constant observable  $\phi_0 \equiv 1$  such that  $\hat{\Phi}(0) = 0$ . According to the presented learning framework in Algorithm 1 with Corollary 3.2, the reduced learning error  $\hat{\zeta}(x, u)$  satisfies

$$\|\hat{\zeta}(x, u)\| = \|\zeta(x, u)\| \leq c_x \|\Phi(x) - \Phi(0)\| + c_u \|u\| = c_x \|\hat{\Phi}(x)\| + c_u \|u\| \quad (36)$$

for all  $x \in \mathbb{X}$  and  $u \in \mathbb{U}$ .

Inspired by the controller designs in [50, 51, 21], we view (35) as an uncertain bilinear system with uncertainty  $\hat{\zeta}(x, u)$ . In particular, we use linear robust control techniques to cope with the uncertainty via convex optimization. More precisely, we define the remainder  $\varepsilon : \mathbb{R}^N \times \mathbb{R}^m \rightarrow \mathbb{R}^N$  depending on the lifted state as

$$\varepsilon(v_1, v_2) = \hat{\zeta}([I_n \quad 0_{n \times N-n}] v_1, v_2). \quad (37)$$

According to the learning error bound (36),  $\varepsilon$  satisfies

$$\|\varepsilon(\hat{\Phi}(x), u)\| = \|\zeta(x, u)\| \leq c_x \|\hat{\Phi}(x)\| + c_u \|u\| \quad (38)$$

for all  $x \in \mathbb{X}$  and  $u \in \mathbb{U}$ . To handle the nonlinear term  $(u \otimes \hat{\Phi}(x))$ , we introduce an artificial uncertainty  $\psi \in \Delta_\Phi$  over-approximating  $\hat{\Phi}(x)$ . This uncertainty needs to be bounded, i.e., we ensure  $\hat{\Phi}(x) \in \Delta_\Phi$  for all times. Then, we stabilize

$$\hat{\Phi}(x_{k+1}) = A\hat{\Phi}(x_k) + B_0u_k + \tilde{B}(I_m \otimes \psi)u_k + \varepsilon(\hat{\Phi}(x), u)$$

for all  $\psi \in \Delta_\Phi$  and perturbation functions  $\varepsilon$  satisfying (38) for all  $x \in \mathbb{X}, u \in \mathbb{U}$ . Setting  $A_K = A + B_0K$ ,  $B_{K_w} = \tilde{B} + B_0K_w$ , and substituting the input by the feedback  $u = \mu_\psi(x) = K\hat{\Phi}(x) + K_w(I_m \otimes \psi)\mu_\psi(x)$ , we obtain the corresponding closed-loop system

$$\hat{\Phi}(x_{k+1}) = A_K\hat{\Phi}(x_k) + B_{K_w}(I_m \otimes \psi)\mu_\psi(x) + \varepsilon(\hat{\Phi}(x), \mu_\psi(x)) \quad (39)$$

with  $\psi \in \Delta_\Phi$  and  $\varepsilon$  satisfying (38) for all  $x \in \mathbb{X}$ .

The remainder of the proof of Theorem 4.1 proceeds similarly to [21, Thm. 7] with the key difference of discrete vs. continuous time, and it is included in the following for completeness.

*Proof.* The presented proof is separated into two parts. First, we show that all  $x \in \mathcal{X}_{\text{SOR}}$  satisfy  $\hat{\Phi}(x) \in \Delta_\Phi$ . Second, we conclude safe operation in  $\mathcal{X}_{\text{SOR}}$  by positive invariance of  $\mathcal{X}_{\text{SOR}}$  together with exponential stability of the sampled closed-loop system (6) for all  $\hat{x} \in \mathcal{X}_{\text{SOR}}$ .

*Part I:  $x \in \mathcal{X}_{\text{SOR}}$  implies  $\hat{\Phi}(x) \in \Delta_\Phi$ :* In order to represent the lifted dynamics via (39), we require  $\hat{\Phi}(x) \in \Delta_\Phi$  for all times. To this end, we exploit that

$$\begin{aligned} 0 &\preceq \frac{1}{\nu} \begin{bmatrix} \nu\tilde{R}_z - 1 & -\nu\tilde{S}_z^\top \\ -\nu\tilde{S}_z & \nu\tilde{Q}_z + P \end{bmatrix} = \begin{bmatrix} \tilde{R}_z & -\tilde{S}_z^\top \\ -\tilde{S}_z & \tilde{Q}_z \end{bmatrix} + \frac{1}{\nu} \begin{bmatrix} -1 & 0 \\ 0 & P \end{bmatrix} \\ &= \begin{bmatrix} 0 & I \\ -1 & 0 \end{bmatrix}^\top \begin{bmatrix} \tilde{Q}_z & \tilde{S}_z \\ \tilde{S}_z^\top & \tilde{R}_z \end{bmatrix} \begin{bmatrix} 0 & I \\ -1 & 0 \end{bmatrix} + \begin{bmatrix} 1 & 0 \\ 0 & -I \end{bmatrix}^\top \begin{bmatrix} -\frac{1}{\nu} & 0 \\ 0 & \frac{1}{\nu}P \end{bmatrix} \begin{bmatrix} 1 & 0 \\ 0 & -I \end{bmatrix} \end{aligned}$$

is equivalent to (18) after dividing the inequality by  $\nu$ . We rewrite this inequality as

$$\begin{bmatrix} 0 & I \\ -I & 0 \\ I & 0 \\ 0 & -I \end{bmatrix}^\top \begin{bmatrix} \tilde{Q}_z & \tilde{S}_z & 0 & 0 \\ \tilde{S}_z^\top & \tilde{R}_z & 0 & 0 \\ 0 & 0 & -\frac{1}{\nu} & 0 \\ 0 & 0 & 0 & \frac{1}{\nu}P \end{bmatrix} \begin{bmatrix} 0 & I \\ -1 & 0 \\ 1 & 0 \\ 0 & -I \end{bmatrix} \preceq 0$$

and apply the dualization lemma [63, Lm. 4.9]. As a consequence, we obtain

$$\begin{bmatrix} I & 0 \\ 0 & 1 \\ 0 & 1 \\ I & 0 \end{bmatrix}^\top \begin{bmatrix} Q_z & S_z & 0 & 0 \\ S_z^\top & R_z & 0 & 0 \\ 0 & 0 & -\nu & 0 \\ 0 & 0 & 0 & \nu P^{-1} \end{bmatrix} \begin{bmatrix} I & 0 \\ 0 & 1 \\ 0 & 1 \\ I & 0 \end{bmatrix} \preceq 0,$$

i.e.,

$$\begin{bmatrix} Q_z & S_z \\ S_z^\top & R_z \end{bmatrix} - \nu \begin{bmatrix} -P^{-1} & 0 \\ 0 & 1 \end{bmatrix} \succeq 0.$$

Hence, we recall the definition of  $\Delta_\Phi$  in (16) and deduce  $\hat{\Phi}(x) \in \Delta_\Phi$  for all  $x \in \mathcal{X}_{\text{SOR}}$  by the multiplication from left and right by  $[\hat{\Phi}(x)^\top \ 1]^\top$  and its transpose, respectively, for  $x \in \mathcal{X}_{\text{SOR}}$  (cf. the S-procedure [63, 64]).

*Part II: Safe operation by positive invariance of  $\mathcal{X}_{\text{SOR}}$  and exponential stability:* In the following, we show  $x_+ \in \mathcal{X}_{\text{SOR}}$  for all  $x \in \mathcal{X}_{\text{SOR}}$  to conclude positive invariance of  $\mathcal{X}_{\text{SOR}}$ , where we use  $(x_+, x)$  as a short-hand notation for  $(x_{k+1}, x_k)$ . The obtained safe operating region  $\mathcal{X}_{\text{SOR}}$  will then result as a Lyapunov sublevel set, for which we define the Lyapunov function candidate  $V(x) = \hat{\Phi}(x)^\top P^{-1} \hat{\Phi}(x)$ , i.e., positive invariance can be inferred if  $\Delta V(x) = V(x_+) - V(x) \leq 0$  for all  $x \in \mathcal{X}_{\text{SOR}}$ .

Recall  $A_K = A + B_0K$  and  $B_{K_w} = \tilde{B} + B_0K_w$ . Then, the definitions  $K = LP^{-1}$  and  $K_w = L_w(\Lambda^{-1} \otimes I_N)$  together with twice applying the Schur complement (cf. [64]) to (17) yields

$$\begin{aligned} & \begin{bmatrix} P - \tau I_N & -B_{K_w}(\Lambda \otimes \tilde{S}_z) & 0 \\ -(\Lambda \otimes \tilde{S}_z^\top)B_{K_w}^\top & H_{K_w} & -(\Lambda \otimes \tilde{S}_z^\top) \begin{bmatrix} 0 \\ K_w \end{bmatrix}^\top \\ 0 & -\begin{bmatrix} 0 \\ K_w \end{bmatrix}(\Lambda \otimes \tilde{S}_z) & 0.5\tau \begin{bmatrix} c_x^{-2}I_N & 0 \\ 0 & c_u^{-2}I_m \end{bmatrix} \end{bmatrix} - \begin{bmatrix} A_K \\ K \\ I \\ K \end{bmatrix} P \begin{bmatrix} A_K \\ K \\ I \\ K \end{bmatrix}^\top \\ & + \begin{bmatrix} B_{K_w}(\Lambda \otimes I_N) \\ K_w(\Lambda \otimes I_N) \\ 0 \\ -K_w(\Lambda \otimes I_N) \end{bmatrix} (\Lambda^{-1} \otimes \tilde{Q}_z) \begin{bmatrix} B_{K_w}(\Lambda \otimes I_N) \\ K_w(\Lambda \otimes I_N) \\ 0 \\ -K_w(\Lambda \otimes I_N) \end{bmatrix}^\top \succ 0, \quad (40) \end{aligned}$$

where  $H_{K_w} = (\Lambda \otimes \tilde{R}_z) - K_w(\Lambda \otimes \tilde{S}_z) - (\Lambda \otimes \tilde{S}_z^\top)K_w^\top$ . We split the obtained matrix into three parts which we factor as

$$\begin{aligned} & \begin{bmatrix} P & 0 & 0 \\ 0 & 0 & 0 \\ 0 & 0 & 0 \end{bmatrix} - \begin{bmatrix} A_K \\ K \\ I \\ K \end{bmatrix} P \begin{bmatrix} A_K \\ K \\ I \\ K \end{bmatrix}^\top = \begin{bmatrix} A_K & -I \\ K & 0 \\ I & 0 \\ K & 0 \end{bmatrix} \begin{bmatrix} -P & 0 \\ 0 & P \end{bmatrix} \begin{bmatrix} A_K & -I \\ K & 0 \\ I & 0 \\ K & 0 \end{bmatrix}^\top, \\ & \begin{bmatrix} 0 & -B_{K_w}(\Lambda \otimes \tilde{S}_z) & 0 \\ -(\Lambda \otimes \tilde{S}_z^\top)B_{K_w}^\top & H_{K_w} & -(\Lambda \otimes \tilde{S}_z^\top) \begin{bmatrix} 0 \\ K_w \end{bmatrix}^\top \\ 0 & -\begin{bmatrix} 0 \\ K_w \end{bmatrix}(\Lambda \otimes \tilde{S}_z) & 0 \end{bmatrix} \\ & + \begin{bmatrix} B_{K_w} \\ K_w \\ 0 \\ -K_w \end{bmatrix} (\Lambda \otimes \tilde{Q}_z) \begin{bmatrix} B_{K_w} \\ K_w \\ 0 \\ -K_w \end{bmatrix}^\top = \begin{bmatrix} B_{K_w} & 0 \\ K_w & -I \\ 0 & 0 \\ K_w & 0 \end{bmatrix} \begin{bmatrix} \Lambda \otimes \tilde{Q}_z & \Lambda \otimes \tilde{S}_z \\ \Lambda \otimes \tilde{S}_z^\top & \Lambda \otimes \tilde{R}_z \end{bmatrix} \begin{bmatrix} B_{K_w} & 0 \\ K_w & -I \\ 0 & 0 \\ K_w & 0 \end{bmatrix}^\top, \end{aligned}$$

and

$$\begin{bmatrix} -\tau I_N & 0 & 0 \\ 0 & 0 & 0 \\ 0 & 0 & 0.5\tau \begin{bmatrix} c_x^{-2}I_N & 0 \\ 0 & c_u^{-2}I_m \end{bmatrix} \end{bmatrix} = \tau \begin{bmatrix} I & 0 \\ 0 & 0 \\ 0 & -I \end{bmatrix} \Pi_r^{-1} \begin{bmatrix} I & 0 \\ 0 & 0 \\ 0 & -I \end{bmatrix}^\top$$

with

$$\Pi_r = \begin{bmatrix} -I_N & 0 \\ 0 & 2 \begin{bmatrix} c_x^2 I_N & 0 \\ 0 & c_u^2 I_m \end{bmatrix} \end{bmatrix}, \quad \Pi_r^{-1} = \begin{bmatrix} -I_N & 0 \\ 0 & 0.5 \begin{bmatrix} c_x^{-2} I_N & 0 \\ 0 & c_u^{-2} I_m \end{bmatrix} \end{bmatrix}.$$

This allows us to write (40) equivalently as

$$\begin{bmatrix} A_K^\top & K^\top & \begin{bmatrix} I \\ K \end{bmatrix}^\top \\ -I & 0 & 0 \\ \hline B_{K_w}^\top & K_w^\top & \begin{bmatrix} 0 \\ K_w \end{bmatrix}^\top \\ 0 & -I & 0 \\ \hline I & 0 & 0 \\ 0 & 0 & -I \end{bmatrix}^\top \begin{bmatrix} -P & 0 & 0 & 0 & 0 & 0 \\ 0 & P & 0 & 0 & 0 & 0 \\ \hline 0 & 0 & \Lambda \otimes \tilde{Q}_z & \Lambda \otimes \tilde{S}_z & 0 & 0 \\ 0 & 0 & \Lambda \otimes \tilde{S}_z^\top & \Lambda \otimes \tilde{R}_z & 0 & 0 \\ \hline 0 & 0 & 0 & 0 & \tau \Pi_r^{-1} & 0 \\ 0 & 0 & 0 & 0 & 0 & 0 \end{bmatrix} \begin{bmatrix} A_K^\top & K^\top & \begin{bmatrix} I \\ K \end{bmatrix}^\top \\ -I & 0 & 0 \\ \hline B_{K_w}^\top & K_w^\top & \begin{bmatrix} 0 \\ K_w \end{bmatrix}^\top \\ 0 & -I & 0 \\ \hline I & 0 & 0 \\ 0 & 0 & -I \end{bmatrix} \succ 0.$$

Applying again the dualization lemma [63, Lm. 4.9] yields

$$\begin{bmatrix} I & 0 & 0 \\ A_K & B_{K_w} & I \\ 0 & I & 0 \\ K & K_w & 0 \\ 0 & 0 & I \\ \begin{bmatrix} I \\ K \end{bmatrix} & \begin{bmatrix} 0 \\ K_w \end{bmatrix} & 0 \end{bmatrix}^\top \left[ \begin{array}{ccc|cc} -P^{-1} & 0 & 0 & 0 & 0 \\ 0 & P^{-1} & 0 & 0 & 0 \\ \hline 0 & 0 & \Lambda^{-1} \otimes Q_z & \Lambda^{-1} \otimes S_z & 0 \\ 0 & 0 & \Lambda^{-1} \otimes S_z^\top & \Lambda^{-1} \otimes R_z & 0 \\ \hline 0 & 0 & 0 & 0 & \tau^{-1} \Pi_r \\ 0 & 0 & 0 & 0 & \end{array} \right] \begin{bmatrix} I & 0 & 0 \\ A_K & B_{K_w} & I \\ 0 & I & 0 \\ K & K_w & 0 \\ 0 & 0 & I \\ \begin{bmatrix} I \\ K \end{bmatrix} & \begin{bmatrix} 0 \\ K_w \end{bmatrix} & 0 \end{bmatrix} < 0, \quad (41)$$

where we refer to the discussion in [63, Sec. 8.1.2] for details on how to build the outer matrices and exploit

$$\begin{bmatrix} \Lambda \otimes \tilde{Q}_z & \Lambda \otimes \tilde{S}_z \\ \Lambda \otimes \tilde{S}_z^\top & \Lambda \otimes \tilde{R}_z \end{bmatrix}^{-1} = \begin{bmatrix} \Lambda^{-1} \otimes Q_z & \Lambda^{-1} \otimes S_z \\ \Lambda^{-1} \otimes S_z^\top & \Lambda^{-1} \otimes R_z \end{bmatrix},$$

according to [51, Thm. 4 (proof)]. Then, we multiply (41) from the left and from the right by  $\begin{bmatrix} \hat{\Phi}(x)^\top & (\mu_\psi(x) \otimes \psi)^\top & \varepsilon(\hat{\Phi}(x), \mu_\psi(x))^\top \end{bmatrix}^\top$  and its transpose, respectively, where  $x \in \mathcal{X}_{\text{SOR}}$ ,  $\mu_\psi(x) = K\hat{\Phi}(x) + K_w(\mu_\psi(x) \otimes \psi)$ ,  $\psi \in \mathbf{\Delta}_\Phi$ , and  $\varepsilon(\hat{\Phi}(x), \mu_\psi(x))$  satisfies (38). This results in

$$\begin{aligned} & [\star]^\top \begin{bmatrix} -P^{-1} & 0 \\ 0 & P^{-1} \end{bmatrix} \begin{bmatrix} \hat{\Phi}(x) \\ A_K \hat{\Phi}(x) + B_{K_w}(\mu_\psi(x) \otimes \psi) + \varepsilon(\hat{\Phi}(x), \mu_\psi(x)) \end{bmatrix} \\ & + [\star]^\top \begin{bmatrix} \Lambda^{-1} \otimes Q_z & \Lambda^{-1} \otimes S_z \\ \Lambda^{-1} \otimes S_z^\top & \Lambda^{-1} \otimes R_z \end{bmatrix} \begin{bmatrix} (I_m \otimes \psi) \mu_\psi(x) \\ K \hat{\Phi}(x) + K_w(\mu_\psi(x) \otimes \psi) \end{bmatrix} \\ & + \tau^{-1} [\star]^\top \Pi_r \begin{bmatrix} \varepsilon(\hat{\Phi}(x), \mu_\psi(x)) \\ \hat{\Phi}(x) \\ K \hat{\Phi}(x) + K_w(\mu_\psi(x) \otimes \psi) \end{bmatrix} < 0. \quad (42) \end{aligned}$$

Here, the second summand of (42) is nonnegative as

$$\mu_\psi(x)^\top \begin{bmatrix} I_m \otimes \psi \\ I_m \end{bmatrix}^\top \begin{bmatrix} \Lambda^{-1} \otimes Q_z & \Lambda^{-1} \otimes S_z \\ \Lambda^{-1} \otimes S_z^\top & \Lambda^{-1} \otimes R_z \end{bmatrix} \begin{bmatrix} I_m \otimes \psi \\ I_m \end{bmatrix} \mu_\psi(x) \geq 0$$

for any  $\psi \in \mathbf{\Delta}_\Phi$  according to the definition of  $\mathbf{\Delta}_\Phi$  in (16) with [51, Prop. 2]. Moreover, the last summand in (42) is nonnegative as

$$\begin{aligned} & [\star]^\top \Pi_r \begin{bmatrix} \varepsilon(\hat{\Phi}(x), \mu_\psi(x)) \\ \hat{\Phi}(x) \\ K \hat{\Phi}(x) + K_w(\mu_\psi(x) \otimes \psi) \end{bmatrix} = 2(c_x^2 \|\hat{\Phi}(x)\|^2 + c_u^2 \|\mu_\psi(x)\|^2) - \|\varepsilon(\hat{\Phi}(x), \mu_\psi(x))\|^2 \\ & \geq (c_x \|\hat{\Phi}(x)\| + c_u \|\mu_\psi(x)\|)^2 - \|\varepsilon(\hat{\Phi}(x), \mu_\psi(x))\|^2 \geq 0. \end{aligned}$$

Hence, we can write (42) as

$$\left( \star \right)^\top P^{-1} \left( A_K \hat{\Phi}(x) + B_{K_w}(\mu_\psi(x) \otimes \psi) + \varepsilon(\hat{\Phi}(x), \mu_\psi(x)) \right) - \hat{\Phi}(x)^\top P^{-1} \hat{\Phi}(x) < 0 \quad (43)$$

if  $x \in \mathcal{X}_{\text{SOR}} \setminus \{0\}$ ,  $\psi \in \mathbf{\Delta}_\Phi$ , and if  $\varepsilon(\hat{\Phi}(x), \mu_\psi(x))$  satisfies (38) (compare, again, with the S-procedure [63, 64]).

Now, we recall the Lyapunov candidate function  $V(x) = \hat{\Phi}(x)^\top P^{-1} \hat{\Phi}(x)$  and verify its satisfaction of  $V(0) = 0$  and

$$\begin{aligned} V(x) & \leq \sigma_{\max}(P^{-1}) \|\hat{\Phi}(x)\|^2 \leq \sigma_{\max}(P^{-1}) L_\Phi^2 \|x\|^2, \\ V(x) & \geq \sigma_{\min}(P^{-1}) \|\hat{\Phi}(x)\|^2 \geq \sigma_{\min}(P^{-1}) \|x\|^2 \end{aligned}$$

due to  $\|\hat{\Phi}(x)\| = \|\Phi(x) - \Phi(0)\|$  and (5). Then, we substitute (39) in (43), i.e., we use  $\hat{\Phi}(x_+) = A_K \hat{\Phi}(x) + B_{K_w}(\mu_\psi(x) \otimes \psi) + \varepsilon(\hat{\Phi}(x), \mu_\psi(x))$ . This yields

$$\Delta V(x) = V(x_+) - V(x) = \hat{\Phi}(x_+)^\top P^{-1} \hat{\Phi}(x_+) - \hat{\Phi}(x)^\top P^{-1} \hat{\Phi}(x) < 0 \quad (44)$$

if  $x \in \mathcal{X}_{\text{SOR}} \setminus \{0\}$ ,  $\psi \in \Delta_{\Phi}$ , and if  $\varepsilon(\hat{\Phi}(x), \mu_{\psi}(x))$  satisfies (38). Hence, the controller  $\mu_{\psi}(x) = K\hat{\Phi}(x) + K_w(\mu_{\psi}(x) \otimes \Delta_{\Phi})$  guarantees (44) for solutions of the lifted system (39) if  $x \in \mathcal{X}_{\text{SOR}} \setminus \{0\}$ ,  $\psi \in \Delta_{\Phi}$ , and if  $\varepsilon(\hat{\Phi}(x), \mu_{\psi}(x))$  satisfies (38). As proven in Part I, we have  $\hat{\Phi}(x) \in \Delta_{\Phi}$  for all  $x \in \mathcal{X}_{\text{SOR}}$ . Further,  $\varepsilon(\hat{\Phi}(x), \mu(x)) = \hat{\zeta}(x, \mu(x))$  due to (37). Consequently, the controller

$$\mu(x) = \mu_{\psi=\hat{\Phi}(x)}(x) = K\hat{\Phi}(x) + K_w(I_m \otimes \hat{\Phi}(x))\mu(x) = (I - K_w(I_m \otimes \hat{\Phi}(x)))^{-1}K\hat{\Phi}(x)$$

renders  $\mathcal{X}_{\text{SOR}}$  positive invariant by guaranteeing (44) in particular for system (35) for all  $x \in \mathcal{X}_{\text{SOR}} \setminus \{0\}$  if  $\hat{\zeta}(x, \mu(x))$  satisfies (36). Moreover, we deduce robust exponential stability of (35) for all  $x \in \mathcal{X}_{\text{SOR}}$  if  $\hat{\zeta}(x, \mu(x))$  satisfies (36).

Finally, we exploit the certificates of SafEDMD in Corollary 3.2, i.e., we deduce that the data-driven surrogates  $K_{\Delta t, d}^{\bar{u}}$ ,  $\bar{u} \in \{0, e_1, \dots, e_m\}$ , and the resulting learning error  $\hat{\zeta}(x, \mu(x))$  of the certified learning scheme in Section 3 satisfy the obtained learning error bound (15) for a data length  $d \geq d_0$  with probability  $1 - \delta$ . Hence, we conclude safe operation by exponential stability of the sampled nonlinear system (6) for all  $x \in \mathcal{X}_{\text{SOR}}$  with probability  $1 - \delta$ .  $\square$

## C Proof of Corollary 4.2

In the following, we prove the stability certificates in Corollary 4.2 for the continuous-time system (1) in closed loop with the sampling-based controller (20).

*Proof.* This is a direct consequence of Theorem 4.1, where we exploit similar arguments as in [52, Thm. 2.27] to infer stability guarantees for the continuous-time system (1) based on the sampled controller (20). In order to show the statement, we need the solutions of the sampled-data closed-loop system to be uniformly bounded over  $\Delta t$  as defined in [52, Def. 2.24], i.e., we have to show the existence of a  $\mathcal{K}$ -function<sup>5</sup>  $\gamma$  such that for all  $\hat{x} \in \mathcal{X}_{\text{SOR}}$ , the solutions of the nonlinear system (1) satisfy

$$\|x(\tau; \hat{x}, \mu_s(x))\| \leq \gamma(\|\hat{x}\|) \quad (45)$$

for all  $\tau \in [0, \Delta t]$ . Note that the sampled controller  $\mu_s(x)$  yields a constant value  $\mu_s(x(\tau)) \equiv \bar{\mu} \in \mathbb{U}$  for  $\tau \in [0, \Delta t]$ . Thus, we observe

$$\|x(\tau; \hat{x}, \bar{\mu})\| \leq \max_{\bar{u} \in \mathbb{U}} \|x(\tau; \hat{x}, \bar{u})\| \stackrel{(5)}{\leq} \max_{\bar{u} \in \mathbb{U}} \|\Phi(x(\tau; \hat{x}, \bar{u})) - \Phi(0)\|$$

for all  $\tau \in [0, \Delta t]$  with  $u(t) \equiv \bar{u}$  on  $[0, \Delta t]$ . Further, recalling  $\phi_0 \equiv 1$  and, hence,  $\mathcal{K}_{\tau}^u \Phi(0) = \Phi(0)$ , we deduce

$$\Phi(x(\tau; \hat{x}, \bar{u})) - \Phi(0) \stackrel{(2)}{=} \mathcal{K}_{\tau}^u \Phi(\hat{x}) - \mathcal{K}_{\tau}^u \Phi(0) = e^{\tau \mathcal{L}^{\bar{u}}} (\Phi(\hat{x}) - \Phi(0))$$

for all  $\tau \in [0, \Delta t]$ . Then,

$$\|x(\tau; \hat{x}, \bar{\mu})\| \leq e^{\Delta t \|\mathcal{L}^*\|} \|\Phi(\hat{x}) - \Phi(0)\| \stackrel{(5)}{\leq} e^{\Delta t \|\mathcal{L}^*\|} L_{\Phi} \|\hat{x}\|$$

where  $\|\mathcal{L}^*\| := \max_{\bar{u} \in \mathbb{U}} \|\mathcal{L}^{\bar{u}}\|$ . Hence, (45) holds for the linear function  $\gamma(r) := cr$  with  $c := e^{\Delta t \|\mathcal{L}^*\|} L_{\Phi}$ . Moreover, exponential stability of the sampled system guarantees the existence of  $C \geq 1$  and  $\sigma \in (0, 1)$  such that  $\|x(k\Delta t)\| \leq C\sigma^k \|\hat{x}\|$  holds for all  $k \geq 0$ , which corresponds to the  $\mathcal{KL}$ -function<sup>6</sup>  $\beta(r, k) = C\sigma^k r$ . Hence, for any  $t \in [k\Delta t, (k+1)\Delta t]$  with  $k \geq 0$  we get

$$\|x(t; \hat{x}, \mu_s(x))\| \leq \gamma(\|x(k\Delta t; \hat{x}, \bar{\mu}_k)\|) \leq \gamma(\beta(\|\hat{x}\|, k)) \leq cC\sigma^k \|\hat{x}\| \leq \tilde{C}e^{-t\eta} \|\hat{x}\|$$

for  $\bar{\mu}_k = \mu_s(x(k\Delta t))$  and with  $\eta := -\ln(\sigma)\Delta t^{-1} > 0$  and  $\tilde{C} := cC\sigma^{-1}$ , i.e., exponential stability of the continuous-time closed-loop system.  $\square$

<sup>5</sup>We denote the class of functions  $\alpha : \mathbb{R}_{\geq 0} \rightarrow \mathbb{R}_{\geq 0}$ , which are continuous, strictly increasing, and satisfy  $\alpha(0) = 0$  by  $\mathcal{K}$ .

<sup>6</sup>A continuous function  $\beta : \mathbb{R}_{\geq 0} \times \mathbb{R}_{\geq 0} \rightarrow \mathbb{R}_{\geq 0}$  belongs to class  $\mathcal{KL}$  if  $\beta(\cdot, s) \in \mathcal{K}$  for each fixed  $s$  and  $\beta(r, \cdot)$  is decreasing with  $\lim_{s \rightarrow \infty} \beta(r, s) = 0$  for each fixed  $r$ .

## D Further details on the numerical experiments in Section 5

In the following, we provide further details on the conducted numerical experiments. Moreover, we define the state-of-the-art Koopman learning EDMDc method for controlled systems and the LQR controller used for comparison.

**Nonlinear inverted pendulum** The inverted pendulum can be modeled via the two-dimensional state  $x = (\theta, \dot{\theta})$  with system dynamics

$$\ddot{\theta}(t) = \frac{g}{l} \sin(\theta(t)) - \frac{b}{ml^2} \dot{\theta}(t) + \frac{1}{ml^2} u(t)$$

with mass  $m$ , length  $l$ , rotational friction coefficient  $b$ , and gravitational constant  $g = 9.81$  m/s. Our experiments are performed with  $m = 1$ ,  $l = 1$ , and  $b = 0.01$ .

**Nonlinear system with Koopman invariant observables** We consider the nonlinear benchmark example

$$\begin{aligned} \dot{x}_1(t) &= \rho x_1(t), \\ \dot{x}_2(t) &= \lambda(x_2(t) - x_1(t)^2) + u(t) \end{aligned}$$

with  $\rho, \lambda \in \mathbb{R}$ , where our simulations are conducted for  $\rho = -2$  and  $\lambda = 1$ . This example permits the definition of an invariant dictionary [32]. In particular, the observable function  $\hat{\Phi}(x) = \left[ x_1 \quad x_2 \quad x_2 - \frac{\lambda}{\lambda - 2\rho} x_1^2 \right]^\top$  leads to *exact* finite-dimensional lifted continuous-time dynamics

$$\frac{d}{dt} \hat{\Phi}(x(t)) = \begin{bmatrix} \rho & 0 & 0 \\ 0 & 2\rho & \lambda - 2\rho \\ 0 & 0 & \lambda \end{bmatrix} \hat{\Phi}(x(t)) + \begin{bmatrix} 0 \\ 1 \\ 1 \end{bmatrix} u(t). \quad (46)$$

Here, even though  $\Phi$  is Koopman-invariant and (46) is exact, the formulation is exposed to a major drawback: The lifted dynamics are time-continuous, i.e., information on the state derivative is necessary in order to learn the exact continuous-time dynamics from data. In particular, the derivative data either needs to be measured directly or estimated based on sample data. This, however, introduces errors (in particular in the presence of noise) and, thus, prevents safe and reliable learning of the underlying true system. Contrary, the proposed SafEDMD learning provides a reliable surrogate model purely based on sample data of state  $x$  and, particularly, without the need for derivative data.

**EDMDc with linear quadratic regulation** As defined in [32, 10], EDMDc relies on the lifted Koopman model

$$\hat{\Phi}_+ \approx \check{A} \hat{\Phi} + \check{B} u, \quad (47)$$

where  $\check{A}$  and  $\check{B}$  are obtained via the linear regression

$$\min_{\check{A}, \check{B}} \left\| \begin{bmatrix} \hat{\Phi}(X_+^0) & \hat{\Phi}(X_+^{e_1}) & \dots & \hat{\Phi}(X_+^{e_m}) \end{bmatrix} - [\check{A} \quad \check{B}] \begin{bmatrix} \hat{\Phi}(X^0) & \hat{\Phi}(X^{e_1}) & \dots & \hat{\Phi}(X^{e_m}) \\ 0_{m \times d^0} & \mathbf{1}_{d^{e_1}}^\top \otimes e_1 & \dots & \mathbf{1}_{d^{e_m}}^\top \otimes e_m \end{bmatrix} \right\|,$$

where  $\mathbf{1}_d \in \mathbb{R}^d$  denotes a vector containing ones. Based on that, a commonly employed control strategy is the discrete-time LQR controller  $\mu_{\text{LQR}} = \check{K} \hat{\Phi}(x)$  for the lifted surrogate model, where

$$\check{K} = -(R + \check{B}^\top \check{P} \check{B})^{-1} \check{B}^\top \check{P} \check{A} \quad (48)$$

with  $\check{P}$  denoting the solution to the discrete-time algebraic Riccati equation

$$\check{P} = \check{A}^\top \check{P} \check{A} - \check{A}^\top \check{P} \check{B} (R + \check{B}^\top \check{P} \check{B})^{-1} \check{B}^\top \check{P} \check{A} + Q.$$

Here,  $Q$  and  $R$  need to be positive definite, and we choose  $Q = R = I$  for simplicity.

We emphasize that the obtained model (47) has no certificates on its learning quality or error. As a consequence, the controller  $\mu_{\text{LQR}}$  is not guaranteed to reliably stabilize the origin of the underlying nonlinear system.